

# Intergenerational Risk Sharing in a Collective Defined-Contribution Pension System: A Simulation Study with Bayesian Optimization

An Chen<sup>\*</sup>, Motonobu Kanagawa<sup>†</sup>, and Fangyuan Zhang<sup>‡</sup>

June 28, 2021

## Abstract

Pension reform is a crucial societal problem in many countries, and traditional pension schemes, such as Pay-As-You-Go and Defined-Benefit schemes, are being replaced by more sustainable ones. One challenge for a public pension system is the management of a systematic risk that affects all individuals in one generation (e.g., that caused by a worse economic situation). Such a risk cannot be diversified within one generation, but may be reduced by sharing with other (younger and/or older) generations, i.e., by *intergenerational risk sharing (IRS)*. In this work, we investigate IRS in a Collective Defined-Contribution (CDC) pension system. We consider a CDC pension model with overlapping multiple generations, in which a funding-ratio-liked declaration rate is used as a means of IRS. We perform an extensive simulation study to investigate the mechanism of IRS. One of our main findings is that the IRS works particularly effectively for protecting pension participants in the worst scenarios of a tough financial market. Apart from these economic contributions, we make a simulation-methodological contribution for pension studies by employing *Bayesian optimization*, a modern machine learning approach to black-box optimization, in systematically searching for optimal parameters in our pension model.

---

<sup>\*</sup>Institute of Insurance Science, Ulm University, Germany, an.chen@uni-ulm.de.

<sup>†</sup>Data Science Department, EURECOM, France, motonobu.kanagawa@eurecom.fr.

<sup>‡</sup>Institute of Insurance Science, Ulm University, Germany. (Corresponding: zhang.fangyuan@uni-ulm.de)

# 1 Introduction

Pension reform is a crucial societal problem in many countries. Traditional pension schemes, such as Pay-As-You-Go (PAYG) and Defined Benefit (DB) pension systems, are becoming unsustainable because of the potential mismatch of incoming and outgoing cash flows (i.e., contributions from working generations and payments to retirees) driven by economic challenges such as demographic change and long-term low interest rates. Many countries are addressing this unsustainability, e.g., by “de-risking” DB plans (Lin et al., 2015; Kessler, 2019) or by substituting the traditional schemes with *fully or partially funded pension schemes* (e.g, Bodie et al. 1988; Poterba et al. 2007; Broeders et al. 2013; Chen and Delong 2015; Chen and Uzelac 2015).

Defined Contribution (DC) pension plans are a representative example of funded pension schemes. In a pure DC pension plan, retirement saving becomes a matter of individual investment: Each participant chooses her investment plan for retirement saving and pays a contribution to the plan on a regular basis; the retirement benefits are determined by the performance of the invested plan and the contributions. Examples of pure DC plans include the “Individual Retirement Accounts” and the 401(k) plans in the United States (Copeland, 2011).

However, the pure DC scheme has two critical problems as a public pension system. One problem is that each individual needs to bear the investment risk. Not everyone has the ability and time for making a good investment decision (Benartzi and Thaler, 2001). Another problem is that there may be an unavoidable risk common for all individuals belonging to the same generation. For instance, such a risk arises if the working period of this generation largely overlaps with a worse economic period. Pure DC plan participants cannot manage such a systematic risk.

## 1.1 Intergenerational Risk Sharing (IRS)

*Collective Defined Contribution (CDC)* pension schemes with multiple generations can address the key problems of pure DC plans, and thus may be more appropriate as a public pension system. In a CDC plan, each participant pays a fixed contribution to the pension fund on a regular basis. Different from pure DC plans, the CDC fund manages and invests the contributions from all participants together. The retirement benefits of each participant are determined by her accumulated contributions and the fund’s investment performance. As the retirement benefits are essentially a redistribution of accumulated contributions from all participants with different generations, the CDC

scheme can naturally implement *intergenerational risk sharing (IRS)*, i.e., risk sharing among different generations.

The core idea of IRS is as follows. Suppose that one generation (say generation A) suffers more from a worse economic situation than other generations, simply because this generation's working period overlaps largely with the worse economic period. Such a risk cannot be easily diversified within one generation, but may be mitigated by sharing the risk with other generations. For instance, there may be another generation (say generation B) that benefits from a good economic situation more than other generations. By sharing this surplus benefit of generation B with the unfortunate generation A, the risk of this generation A can be reduced.<sup>1</sup>

In the literature on collective pension funds (including CDC funds), IRS has been studied by many researchers. For example, Gollier (2008) theoretically proves that, under a certain assumption, a CDC fund can improve the welfare of all generations (compared to the situation where each generation invests individually and optimally) by enhancing the risk-taking ability of each generation. Beetsma and Bovenberg (2009) consider a two-period overlapping generations model, and show that a collective DB scheme with an appropriate investment policy can achieve the optimal IRS. A simulation study by Cui et al. (2011) shows that a hybrid pension fund (in which both contributions and retirement payments can be adjusted) can achieve the ex-ante Pareto welfare improvement for all generations. Kurtbegu (2018) studies a pension model imitating a Dutch CDC pension fund for the time-horizon of 150 years, and compares it with other pension systems by simulations, concluding that the CDC pension system appears to be the best in terms of the IRS against demographic shocks. The Dutch pension system is an example of CDC pension plans in reality, and more analyses and details of it are available in, e.g., Bovenberg et al. (2007); Nijman et al. (2014); Bovenberg and Nijman (2019); Westerhout (2020).

## 1.2 Contributions

We contribute to the literature by investigating how intergenerational risk sharing can be implemented in CDC pension systems. We consider a CDC pension system with an overlapping generations model. Like pure DC funds, each participant has an "individual benefit account" that keeps track of the asset belonging to this participant. Each participant pays regular fixed contributions to the pension fund, which are collected in the individual benefit account. The pension fund invests its asset (originally the

---

<sup>1</sup>For classical analysis of IRS, see e.g., Diamond (1977); Gordon and Varian (1988); Shiller (1999).

contributions from the participants) in the financial market, and adjusts the *declaration rate*, which determines the growth rate of individual benefit accounts, according to the fund's investment performance. Each participant's retirement benefits are determined by the terminal value of her benefit account at the time of retirement.

For the adjustment of the declaration rate, we use the *funding-ratio-linked declaration rate* studied in Goecke (2013). This approach formulates the declaration rate as a stochastic process depending on the expected log asset return and the funding ratio — the ratio of the fund's asset and liability. For instance, given a good (resp. bad) fund's investment performance, the funding ratio becomes accordingly larger (resp. smaller), and the declaration rate is increased (resp. decreased) so that each participant's benefit account grows more rapidly (resp. more slowly).

In this paper, we study the functionality of the funding-ratio-linked declaration rate as a means of IRS in the CDC pension scheme. Suppose that a worse period in the financial market has started at a certain point of time. As the younger generations' working periods may overlap with the worse period much longer than the older generations, this results in higher risks for the younger generations. In contrast, the worse economic period would result in lower risks for the older generations, since their remaining working periods are shorter and thus their assets are damaged less severely. Therefore in this situation, the IRS should work for sharing the higher risks of the younger generations with the older generations.

The funding-ratio-linked declaration rate automatically achieves this IRS. Suppose that the worse economic situation makes the fund's investment performance worse. Then the declaration rate is automatically decreased, letting each benefit account grow more slowly. This adjustment has a stronger impact on the older working generations, since their retirement dates are closer than for younger generations. It essentially results in pooling some assets from the older generations to redistribute later to the younger generations to reduce their risk. Similar reasoning can be made for a better economic period, in which case younger generations share the risk of older generations.

Our pension model has two parameters that need to be specified: one determining the investment strategy and the other specifying the strength of adjustment in the funding-ratio-linked declaration rate. We determine these two parameters by formulating and solving a maximization problem of the expected utility of a hypothetical social planner. We assume that this social planner takes into account the retirement benefits of all generations including those in the future. Since there is no analytic solution for the maximization problem, we numerically search for the optimal parameters with simulations using *Bayesian optimization*.

We perform an extensive simulation study covering several different settings of i) the degree of relative risk aversion that decides the planner’s attitude towards the risk, and ii) the market price of risk, given as the Sharpe ratio of the expected market return divided by the volatility of the market. We obtain the following observations regarding the functionality on the funding-ratio-linked declaration rate as a mechanism for IRS, which we report in Section 5:

1. The evolution of each individual benefit account becomes much smoother than the corresponding account in a pure DC with the same investment strategy. This is due to the smoothing effect of IRS.
2. IRS works particularly effectively in a tough market where the market price of risk is low. In particular, in worst scenarios of the financial market, the IRS protects the participants from losing too much, compared to the corresponding participants in a pure DC plan.

These observations indicate that the CDC scheme with the funding-ratio-linked declaration rate is promising as a public pension system.

Apart from the above economic contribution, we make a “meta” contribution in terms of simulation methodology for studying pension systems. To numerically optimize the two parameters in our pension model, we use Bayesian Optimization (Shahriari et al., 2016), a modern machine learning approach to optimizing a black-box objective function. The objective function in our case is the mapping from the two parameters to the resulting expected utility. Since it does not have an analytic expression, we numerically approximate the expected utility by the Monte Carlo average over 10,000 simulations of the financial market, where each simulation is over 100 years. As such, one evaluation of our objective function for given candidate parameters is computationally expensive.<sup>2</sup> For the optimization of such an objective function, brute-force approaches such as grid search have been used in the pension literature [e.g., Cui et al. 2011; Bams et al. 2016]. However, grid search is inefficient and requires a large number of function evaluations to obtain a reliable solution. Bayesian optimization is much more efficient than grid search, as it iteratively refines the search space by quantifying the uncertainty of the response surface of the objective function based on evaluated function values. Since Bayesian optimization can result in optimal parameters with a smaller computational budget, this opens up many possibilities for studying more sophisticated but

---

<sup>2</sup>With the authors’ computational environment, one evaluation of the objective function requires a few minutes. Thus, if we evaluate 100 candidate pairs of the two parameters, in total we need more than one or two hours to finish.

more computationally intensive models with many parameters. Thus, our “meta” contribution is to show that Bayesian optimization is a useful tool for simulation studies of pension systems in general.

The paper is organized as follows. Section 2 presents our pension model, and Section 3 describes how Bayesian optimization can be used for selecting the parameters in the pension model. Section 4 studies the optimal parameters obtained for several different settings and the resulting simulation paths. Section 5 investigates the intergenerational risk sharing in our pension model by comparing it to the corresponding pure DC plan. Section 6 concludes. Additional results are reported in the appendix.

### 1.3 Related work

Our work is closely related to a line of research on the IRS in CDC pension models. Baumann and Müller (2008) study the IRS in a CDC pension model using a declaration rate based on the *risk-free* rate adjusted with the funding-ratio process. They analyze the optimal investment strategy from the viewpoint of one generation, and show that the Pareto improvement of the welfare can be achieved, assuming a self-financing continuous model. Goecke (2013) considers a self-financing pension model similar to Baumann and Müller (2008), but with a declaration based on the *expected asset return* adjusted with the funding-ratio process. This funding-ratio-linked declaration rate is what we study in our work. Goecke (2013) analyzes the properties of the resulting funding-ratio process.

One key issue in pension reform is the mismatch of the incoming and outgoing cash flows (i.e., the contributions from working generations and the payments to retirees). Hence, the assumption that the pension fund is self-financing (i.e., there is no mismatch between the cash flows) is not realistic in this regard. There are a few works that extend the self-financing model of Goecke (2013) to more realistic CDC pension funds with multiple generations, e.g., by explicitly modeling cash flows. Bams et al. (2016) consider a CDC pension model with multiple generations similar to ours, in which the declaration rate of Goecke (2013) and a constant-mix investment strategy are used. Donnelly (2017) studies a CDC pension model with multiple generations, in which the investment strategy is adjusted to achieve a target funding-ratio. She shows that the resulting retirement benefits are more stable than those in a corresponding pure DC plan in the sense that their variations become narrower.

We contribute to this line of research by providing novel insights about the functionality of the funding-ratio-linked declaration rate as a means of IRS in a CDC pension

system. By thoroughly studying different settings for the market price of risk of the financial market (captured by the Sharpe ratio) and the risk attitude of the social planner (or the fund manager), we show that the IRS works particularly effectively in worst scenarios of a tough market for protecting the participants. This property, which is desirable for a public pension system, is a new finding about the functionality of the IRS in CDC pension systems. Moreover, our simulation experiments show that the optimal investment strategy and the associated adjustment strength of the declaration rate are highly dependent on the market price of risk of the financial market and the risk attitude of the social planner.

Lastly, we emphasize that the use of Bayesian optimization has enabled our extensive simulation study, as Bayesian optimization can drastically reduce the computational times required. Without using Bayesian optimization, it would have not been possible to obtain the above new findings, as the brute-force approaches such as grid search are too time-consuming with the authors' computational environment.<sup>3</sup> In this sense, our work demonstrates the benefits of using Bayesian optimization, or machine learning in general, in simulation studies of pension systems.

## 2 Model setup

### 2.1 The underlying financial market and pension asset dynamics

To introduce our stylized CDC pension model, we first define the setup. Let  $t \geq 0$  denote a time point, with the unit being one year (i.e.,  $t = 1$  is one year after the pension fund started at time  $t = 0$ ). For the financial market, we consider the Black–Scholes model where there exist a risk-free asset  $F(t) \geq 0$  and a risky asset  $S(t) \geq 0$ , modelled as stochastic processes whose dynamics are given by

$$\begin{aligned} dF(t) &= rF(t)dt, & F(0) &= F_0, \\ dS(t) &= \mu S(t)dt + \sigma S(t)dW(t), & S(0) &= S_0, \end{aligned}$$

---

<sup>3</sup>For grid search to match the accuracy of Bayesian optimization, it usually requires a much larger number of function evaluations and thus is more time-consuming. For example, for grid search, 100 function evaluations amount to  $10 \times 10$  grids (for optimizing two parameters), by which one can only obtain a rough estimate for the optimal solution. If one chooses finer grids of size, say,  $40 \times 40 = 1600$ , one needs 16 times more computational costs. See Figure 3 in Section 3 for an illustration of how grid search can be inefficient compared to Bayesian optimization.

where  $r > 0$  is the risk-free rate,  $\mu > r$  and  $\sigma > 0$  are the constant drift and volatility of the risky asset, respectively. We use  $F_0 > 0$  to denote the initial value of the risk-free asset,  $S_0 > 0$  the initial value of the risky asset, and  $W(t)$  the standard Brownian motion under the real world probability measure.

Denote by  $A(t) \geq 0$  the asset of the pension fund at time  $t \geq 0$ . Assume that, at time  $t$ , the fund invests the fraction  $\pi(t) \geq 0$  of its asset  $A(t)$  into the risky asset  $S(t)$ , and the rest  $1 - \pi(t)$  into the risk-free asset  $F(t)$ . Then, the dynamics of the asset  $A(t)$  as a stochastic process is given by

$$\begin{aligned} dA(t) &= \pi(t)A(t)\frac{dS(t)}{S(t)} + (1 - \pi(t))A(t)\frac{dF(t)}{F(t)} \\ &= A(t) [(\pi(t)(\mu - r) + r)dt + \pi(t)\sigma dW(t)], \quad A(0) = a_0, \end{aligned} \quad (2.1)$$

where  $a_0 > 0$  is the initial asset of the fund. The constraint  $\pi(t) \geq 0$  means that short selling ( $\pi(t) < 0$ ) is prohibited. This is consistent with regulations on pension funds' investment policies in reality.

We describe the basis scheme of our pension model. We consider an overlapping generations model (OLG model) consisting of  $N \in \mathbb{N}$  working generations (e.g.,  $N = 40$  generations of people of ages from 25 to 64). We assume, for simplicity, that each generation consists of one hypothetical participant<sup>4</sup>. At the beginning of each year  $t = 0, 1, 2, \dots$ , the oldest working generation leaves the fund and a new youngest generation joins it. As a consequence, there are always  $N$  working generations in the fund. The fund pays lump-sum benefits  $B(t) > 0$  to the generation who has just retired, where  $B(t)$  is determined by their benefit accounts, introduced below. At the same time, each of  $N$  working generations pays a fixed amount  $y > 0$  to the fund as a contribution. Thus, the cash flows (of the contributions from the  $N$  working generations and the payments to the retired generation) occur at discrete time points  $t = 0, 1, 2, \dots$  in our model, while the asset  $A(t)$  changes continuously. This implies that the asset process  $A(t)$  has a jump at the beginning of each year:

$$A(t)_+ = A(t) + \underbrace{Ny}_{\text{Contributions}} - \underbrace{B(t)}_{\text{Payments}}, \quad t = 0, 1, 2, \dots \quad (2.2)$$

where  $A(t)_+ := \lim_{\varepsilon \rightarrow +0} A(t + \varepsilon)$  denotes the right continuous limit.

For ease of understanding, we illustrate the cash flows of the pension fund with  $N = 40$  working generations in Figure 1.

---

<sup>4</sup>This essentially represents the situation where each generation consists of about the same number of participants.

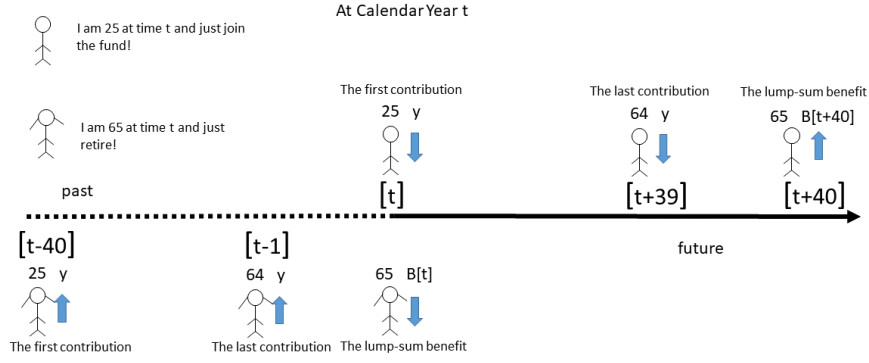


Figure 1: The OLG pension fund with one retired generation.

## 2.2 Individual benefit accounts

We now introduce the *individual benefit account* for each generation. The individual benefit account of one generation may be interpreted as the asset that belongs to this generation, and its value at the retirement date becomes the total amount of benefits to be paid to this generation after retirement. As such, the individual benefit account is determined by the accumulated contributions from the generation and the performance of the pension fund.

**Generation indicators.** To describe this, we need to introduce some notations. Let  $\tau_0 \in \mathbb{N}$  be the age of the youngest working generation (e.g.,  $\tau_0 = 25$ ) and  $\tau_R \in \mathbb{N}$  be the age of the retired generation (e.g.,  $\tau_R = 65$ ). For the generation of age  $\tau \in \mathbb{N}$  at time  $t$ , we then define its unique indicator  $i = i(\tau, t) \in \mathbb{N}$  as

$$i := i(\tau, t) := \tau_R - \tau + [t], \quad \tau \in \mathbb{N}, \quad t \geq 0, \quad (2.3)$$

where  $[t]$  denotes the integer part of  $t$  (e.g., if  $t = 3.4$  then  $[t] = 3$ ). The indicator  $i$  represents the calendar year when this generation retires, as can be seen by setting  $\tau = \tau_R$  in (2.3).

Note that the generation  $i$  of age  $\tau$  at time  $t$  is a working generation if and only if  $\tau_0 \leq \tau < \tau_R$ . Since  $\tau = \tau_R + [t] - i$  by the definition of  $i$ , this condition is equivalent to  $\tau_0 \leq \tau_R + [t] - i < \tau_R$ , or  $i - (\tau_R - \tau_0) \leq [t] < i$  by rearranging. Thus, we can define the set of the indicators for *all working generations at time  $t$*  as

$$I_w(t) := \{i \in \mathbb{N} \mid i - (\tau_R - \tau_0) \leq [t] < i\}.$$

It follows that the generation with indicator  $i$  starts being a working generation at time  $t = i - (\tau_R - \tau_0)$  and retires at time  $t = i$ , as mentioned.

**Individual benefit accounts.** We now define individual benefit accounts. Below let  $\tau_i := \tau_R + [t] - i$  denote the age of generation  $i$  at time  $t$ . For generation  $i$ , let  $B_i(t) \geq 0$  denote its individual benefit account at time  $t$ , and we define its dynamics by

$$B_i(i - (\tau_R - \tau_0)) = 0, \quad (2.4)$$

$$dB_i(t) = B_i(t)\eta(t)dt, \quad t \in [i - (\tau_R - \tau_0), i], \quad (2.5)$$

$$B_i(t)_+ = B_i(t) + y, \quad t \in \{i - (\tau_R - \tau_0), i - (\tau_R - \tau_0) + 1, \dots, i - 1\}, \quad (2.6)$$

where  $\eta(t) \in \mathbb{R}$  is the *declaration rate* at time  $t$ , introduced below.

We first explain interpretations of the dynamics of the individual account. The generation  $i$  first becomes a working generation at time  $t = i - (\tau_R - \tau_0)$ , and at this point the individual benefit account  $B_i(t)$  starts from 0 as in (2.4). The benefit account  $B_i(t)$  evolves continuously according to the declaration rate  $\eta(t)$  as in (2.5), and increases with its own contribution  $y$  at the beginning of each year  $t = i - (\tau_R - \tau_0), \dots, i - 1$ , while the generation  $i$  is in the working generations as in (2.6). When the generation  $i$  retires at time  $t = i$ , the fund pays the amount of

$$B(t) = B_i(t) = B_i(i), \quad t \in \mathbb{N} \quad (2.7)$$

as a lump-sum retirement benefit.

**Liability.** We define the liability  $L(t)$  of the fund at time  $t$  endogenously as the sum of the individual benefit account values of all participants:

$$L(t) := \sum_{i \in I_w(t)} B_i(t), \quad t > 0,$$

where  $I_w(t)$  is the set of indicators for all the working generations at time  $t$ . We define the liability in this way, since our fund is of the defined-contribution type and the obligation of the fund is essentially its benefit account values.

Due to the individual benefit accounts  $B_i(t)$  in (2.5) and (2.6), the dynamics of the liability  $L(t)$  is then given by

$$\begin{aligned} dL(t) &= L(t)\eta(t)dt, \quad t \geq 0, \quad L(0) = a_0, \\ L(t)_+ &= L(t) + Ny - B(t), \quad t \in \mathbb{N}, \end{aligned} \quad (2.8)$$

where  $B(t)$  is the payment to the retired generation  $i = t$  at time  $t$  in (2.7). We set the initial value of the liability  $L(0)$  as the initial value of the asset  $A(0) = a_0$ , so that the funding ratio is  $A(0)/L(0) = 1$ .

**Declaration rate.** We now define the declaration rate  $\eta(t)$  in (2.5). Let

$$\mu(t) := \pi(t)(\mu - r) + r - \frac{1}{2}\pi(t)^2\sigma^2$$

be the expected log-return value of the asset  $A(t)$  at time  $t$ , which can be obtained from (2.1). Then we define the declaration rate  $\eta(t)$  at time  $t$  as

$$\eta(t) = \mu(t) + \theta \ln(A(t)/L(t)), \quad (2.9)$$

where  $0 \leq \theta \leq 1$  is an adjusting parameter. That is, the declaration rate  $\eta(t)$  is the expected log-return  $\mu(t)$  adjusted by the logarithm of the funding ratio  $A(t)/L(t)$ .

The adjustment by the funding ratio  $A(t)/L(t)$  works as follows. Inserting the definition of the declaration rate  $\eta(t)$  in (2.5), the continuous dynamics of the individual benefit account  $B_i(t)$  of generation  $i$  is given as

$$dB_i(t) = B_i(t)\eta(t)dt = B_i(t) (\mu(t) + \theta \ln(A(t)/L(t))) dt.$$

Assume that, at time  $t$ , the asset  $A(t)$  is larger than the liability  $L(t)$ :  $A(t) > L(t)$ . Then we have  $\ln(A(t)/L(t)) > 0$ , and thus the declaration rate  $\eta(t)$  becomes larger than the expected log return  $\mu(t)$  because of the adjustment. Accordingly, the individual benefit account  $B_i(t)$  grows faster, and as a result the liability  $L(t)$  also grows faster, as can be seen from (2.8). On the other hand, assume that the asset  $A(t)$  is smaller than the liability  $L(t)$ , i.e.,  $A(t) < L(t)$ . Then we have  $\ln(A(t)/L(t)) < 0$ , and thus the declaration rate  $\eta(t)$  is adjusted to be smaller than the expected return  $\mu(t)$ . In this way, the individual benefit account  $B_i(t)$  grows more slowly, and the resulting liability  $L(t)$  also grows more slowly.

### 2.3 Optimization problem

Having introduced our model, we now define an optimization for finding the investment strategy  $\pi(t)$ ,  $t \geq 0$  in (2.1) and the adjustment parameter  $\theta$  in the declaration rate in (2.9). We consider a hypothetical social planner who runs the pension fund and cares about the benefits of all generations, and define our objective function as the expected utility of this social planner. To this end, let  $U_\gamma : (0, \infty) \rightarrow (-\infty, \infty)$  be

a constant relative risk aversion (CRRA) utility function<sup>5</sup> with relative risk aversion  $\gamma \geq 0$ :

$$U_\gamma(x) := \frac{x^{1-\gamma}}{1-\gamma} \quad (\text{for } \gamma \neq 1), \quad U_\gamma(x) := \ln(x) \quad (\text{for } \gamma = 1). \quad (2.10)$$

We then define our objective function as the expected sum of the discounted utilities (with a subjective discount factor  $\beta \in (0, 1)$ ) of the payments to all the generations. The optimization problem is thus given as:

$$\max \left\{ \mathbb{E} \left[ \sum_{t=0}^{\infty} \beta^t U_\gamma(B(t)) \right] \mid \pi(t) \geq 0, \quad 0 \leq \theta \leq 1, \quad \text{subject to } A(t) > 0 \text{ for all } t \geq 0 \right\}, \quad (2.11)$$

where  $B(t)$  is the pension payment to the retired generation  $i = t$  at time  $t$  in (2.7).

In this work, for the investment strategy  $\pi(t)$  in (2.11), we confine ourselves to a constant mix strategy of the form

$$\pi(t) = \pi \geq 0, \quad \forall t \geq 0.$$

Thus, the optimization problem is with respect to this constant  $\pi$  and the adjustment parameter  $\theta$ . In general, a constant-mix strategy is easy to implement, and hence is a prevailing candidate for a collective pension design, see for example Cui et al. (2011), Goecke (2013) and Bams et al. (2016).

As an analytic solution is not available for our optimization problem, we numerically search for the optimal parameters using *Bayesian optimization*, a modern machine learning approach to black-box optimization, as detailed in the next section.

**Relative risk aversion and investment regulations.** The relative risk aversion  $\gamma$  in our model may be interpreted as capturing a regulation on the pension fund's investment policy, as  $\gamma$  indirectly determines the investment strategy, as we will see in Section 4. According to an annual survey of OECD (2020), investment regulations on pension funds differ among different countries. For example, in countries like the U.S., the U.K., and the Netherlands, there is basically no limitation for pension funds' investment. On the other hand, in countries such as France and Germany, there are relatively conservative upper-limits on the fraction of pension funds' assets to be invested in equity. Since in our model, a larger (resp. smaller)  $\gamma$  leads to a more conservative (resp. aggressive) investment strategy, the choice of  $\gamma$  may be interpreted as indirectly representing the strength of a regulation.

---

<sup>5</sup>See e.g. Chiappori and Paiella (2011) for an empirical study supporting the use of the CRRA utility function.

**Bankruptcy** In our pension model, we define bankruptcy to occur at time  $t$  when the pension's asset becomes non-positive:  $A(t) \leq 0$ . Thus, the constraint  $A(t) > 0$  for all  $t > 0$  in the optimization problem (2.11) is to require that the fund does not go bankrupt. In practice, however, this hard constraint is difficult to satisfy, because of the unboundedness of the Brownian motion defining the financial market. In Section 3, we introduce a soft constraint that encourages the numerically optimized parameters not to lead to bankruptcy.

Note that bankruptcy is usually defined as when the pension's asset is below the pension's liability. However, in our model, the liability is endogenously defined as the sum of the benefit account values of working generations, and is continuously adjusted according to the funding ratio. Thus, this definition of bankruptcy is not appropriate for our pension model. This is why we define bankruptcy as the pension's asset  $A(t)$  being not positive, i.e., when the pension fund's assets are depleted.

## 2.4 Entry cohorts

Here, we discuss the entry cohorts, i.e., the first generations who participate in the fund at time  $t = 0$  when the pension fund starts. Before this period, i.e., when  $t < 0$ , we assume that these entry cohorts maintained their individual benefit accounts  $B_i(t)$  with a pure saving policy (where  $i$  is the indicator of one of the generations in the entry cohorts). In other words, we assume for  $t < 0$  the individual benefit account  $B_i(t)$  for generation  $i$  in the entry cohorts accumulated at the risk-free rate  $r$ :

$$dB_i(t) = rB_i(t)dt, \quad t < 0,$$

and for  $t \geq 0$  it evolves according to our design described in (2.5) (2.6). Hence, we adopt the same way to deal with the entry cohorts as Bams et al. (2016).

## 3 Bayesian optimization (BO)

We explain here the details of *Bayesian optimization (BO)*. As mentioned, we use BO to maximize the expected utility in (2.11), to numerically search for the optimal values of the investment strategy  $\pi$  and adjustment parameter  $\theta$ . BO is a modern machine learning approach to globally optimizing a black-box objective function (Shahriari et al., 2016). For implementation, we use the R package *mlrMBO* (Bischl et al., 2017).

BO has been widely used in applications where the objective function is defined by simulations, and thus where the evaluation of the objective function is computationally expensive. This is our case with the expected utility (2.10), because we approximate the expectation with Monte Carlo simulations. For the optimization of such a black-box objective function, grid search is often used in practice. However, grid search is not efficient and computationally demanding. BO is much more efficient than grid search, as it iteratively refines the search space by taking into account the evaluated function values.

This iterative refinement is enabled by using the so-called *acquisition function*, which suggests the next point to evaluate. The acquisition function is defined on the basis of the learning and uncertainty quantification of the landscape of the objective function. This learning and uncertainty quantification is done by a Bayesian statistical learning approach called *Gaussian process regression* (or Kriging). This is why BO is called “Bayesian.”

We first describe the basic framework of BO in Section 3.1. We then explain Gaussian process regression in Section 3.2 and the acquisition function in Section 3.3. We demonstrate the application of BO in our simulation study in Section 3.4. The readers who are only interested in the economic aspects of the paper can directly move to the next section.

### 3.1 Basic framework

We first describe the basic framework of BO. Let  $\Omega$  be a parameter set and  $f : \Omega \rightarrow \mathbb{R}$  be the objective function to be maximized. In our problem, this parameter set is  $\Omega = [0, 3] \times [0, 1]$  and each  $x := (\pi, \theta) \in \Omega$  represents a pair of the investment strategy  $\pi \geq 0$  and adjustment parameter  $\theta \geq 0$ . We define the objective function as the certainty equivalent (CE) of the expected utility in (2.11) with input parameters  $x = (\pi, \theta)$ :

$$f(x) := f(\pi, \theta) := CE(\pi, \theta), \quad (3.1)$$

$$\text{where } CE(\pi, \theta) \geq 0 \text{ is such that } U_\gamma(CE(\pi, \theta)) = \mathbb{E} \left[ \sum_{t=0}^{\infty} \beta^t U_\gamma(B(t)) \right].$$

Note that the expected utility is a function of  $x = (\pi, \theta)$ , as the payment  $B(t)$  depends on  $\pi$  and  $\theta$ . Since the CRRA utility function  $U_\gamma$  is strictly monotonically increasing with respect to its argument, the maximizer of the certainty equivalent is the same as

the maximizer of the expected utility:

$$\arg \max_{(\pi, \theta) \in \Omega} CE(\pi, \theta) = \arg \max_{(\pi, \theta) \in \Omega} \mathbb{E} \left[ \sum_{t=0}^{\infty} \beta^t U_{\gamma}(B(t)) \right].$$

Thus, the maximization of the expected utility can be equivalently formulated as the maximization of the objective function (3.1).

In our simulation study, the expected utility is approximated by the Monte Carlo average of 10,000 simulations of the asset process  $A(t)$  (and thus the resulting  $B(t)$ ) for  $t = 0, 1, \dots, T := 100$ . Therefore, each evaluation of  $f(x)$  for a given  $x = (\pi, \theta)$  involves 10,000 simulations over 100 years, which is computationally expensive.

**Procedure of Bayesian optimization.** First, we generate initial design points  $x_1, \dots, x_{n_{\text{init}}}$  for some  $n_{\text{init}} \in \mathbb{N}$ , and evaluate the function values  $f(x_1), \dots, f(x_{n_{\text{init}}})$  on these points. One can generate these initial points randomly (e.g., uniform sampling on  $\Omega$ ) or deterministically (e.g., grid points). In our study, we use the design given by Latin hypercube sampling (McKay et al., 2000) on  $\Omega$  with  $n_{\text{init}} = 10$ .

Below we use the notation  $D_n := \{(x_i, f(x_i))\}_{i=1}^n \subset \Omega \times \mathbb{R}$  to write the collection of points  $x_1, \dots, x_n$  and the resulting function values  $f(x_1), \dots, f(x_n)$ .  $D_n$  can be understood as “data” or “observations” about  $f$  after  $n$ -time evaluations of the function. We also denote by  $\alpha(x; D_n)$  the *acquisition function*, whose concrete form will be introduced later in Section 3.3. The acquisition function  $\alpha(x; D_n)$  is a function of  $x \in \Omega$  and defined from  $D_n$ .

BO iterates the following procedure for  $n = n_{\text{init}} + 1, n_{\text{init}} + 2, \dots, N$ , where  $N$  is the total number of function evaluations.

1. Compute  $x_{n+1} \in \arg \max_{x \in \Omega} \alpha(x; D_n)$ ,
2. Simulate  $f(x_{n+1})$ , and augment the data  $D_{n+1} := D_n \cup \{(x_{n+1}, f(x_{n+1}))\}$ .

An estimate of the optimal parameters is then given as the maximizer from the evaluated inputs  $x_1, \dots, x_N$ :

$$x^* \in \arg \max \{f(x) \mid x \in \{x_1, \dots, x_N\}\}$$

The acquisition function  $\alpha(x; D_n)$  determines the next point  $x_{n+1}$  to evaluate the objective function  $f$ . Note that the computational cost of solving  $\max_{x \in \Omega} \alpha(x; D_n)$  is negligible compared to the computational cost of evaluating  $f(x_{n+1})$ , as  $\alpha(x; D_n)$  can be evaluated cheaply.

The acquisition function is designed so as to balance the *exploitation* and *exploration*. Exploitation is a strategy to search for in a region near the current maximizer in  $x_n^* := \arg \max\{f(x) \mid x \in \{x_1, \dots, x_n\}\}$ ; exploration is to search for in a region far from the evaluated points  $x_1, \dots, x_n$ . This *exploration-exploitation trade-off* is enabled by the learning and uncertainty quantification of the response surface of  $f$  from the data  $D_n$ . This is done by Gaussian process regression, which we will explain next.

### 3.2 Gaussian process regression

Gaussian process regression (Rasmussen and Williams, 2006) is a Bayesian non-parametric method for learning (or approximating) an unknown function  $f : \Omega \rightarrow \mathbb{R}$  from its finite observations (data)  $D_n = \{(x_i, f(x_i))\}_{i=1}^n$ . Recall that Bayesian inference in general proceeds as follows: a) define a *prior distribution* for the quantity of interest, b) collect observations (data) related to that quantity, and c) update the prior distribution to the *posterior distribution* using the observed data, applying Bayes' rule. In Gaussian process regression, the quantity of interest is the unknown *function*  $f$ , and a') one defines a prior distribution of  $f$  as a Gaussian process (or Gaussian random field), b') collects data  $D_n = \{(x_i, f(x_i))\}_{i=1}^n$ , and c') updates the prior Gaussian process to the *posterior* Gaussian process, applying Bayes' rule. See Figure 2 for illustrations of Gaussian process regression.

**Prior Gaussian process.** A Gaussian process is completely specified by its *mean function*  $m : \Omega \rightarrow \mathbb{R}$  and *covariance function*  $k : \Omega \times \Omega$ . We write  $f \sim \mathcal{GP}(m, k)$  to mean that  $f$  is a sample path of the Gaussian process with mean function  $\mu$  and covariance function  $k$ . Then we have  $\mu(x) = \mathbb{E}[f(x)]$ ,  $x \in \Omega$  and  $k(x, x') = \mathbb{E}[(f(x) - \mu(x))(f(x') - \mu(x'))]$ ,  $x, x' \in \Omega$ . By specifying  $\mu$  and  $k$ , we implicitly specify the corresponding Gaussian process.

For simplicity, we consider a Gaussian process with the zero-mean function (i.e.,  $\mu(x) = 0, \forall x \in \Omega$ ) for our prior distribution of the objective function  $f$ :

$$f \sim \mathcal{GP}(0, k). \quad (3.2)$$

What we need is to specify the covariance function  $k$ . By doing so, we can express our assumption or knowledge regarding key properties of the objective function  $f$ , such as its smoothness and structure.

Popular choices of covariance kernels include square-exponential kernel  $k(x, x') = \exp(-\|x - x'\|^2/h)$  with  $h > 0$  and *Matérn kernels*. In our study we use the so-called

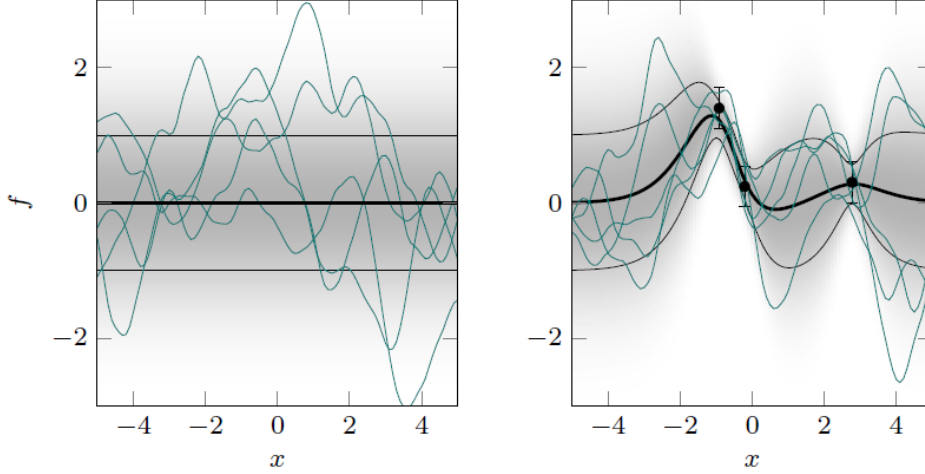


Figure 2: Illustrations of Gaussian process regression, adapted from Kanagawa et al. (2018, Figure 1). **Left:** The green curves are 5 sample paths from the prior Gaussian process (3.2) using the Matérn kernel (3.3) with  $h = 1$ . The thick black line is the prior mean function  $m(x) = 0$ . **Right:** the three points are noise-perturbed observations  $(x_i, y_i)_{i=1}^3$ , where  $y_i = f^*(x_i) + \varepsilon_i$  with  $f^*$  being the ground-truth function and  $\varepsilon_i$  being an independent zero-mean Gaussian noise with variance  $\sigma^2 := 0.01$ . The thick black curve is the posterior mean function  $m_n(x)$  in (3.5) and the two thin black curves are the posterior standard deviation function  $\sigma_n(x) = \sqrt{k_n(x, x)}$  in (3.7), in which  $\mathbf{K}_n^{-1}$  is replaced by  $(\mathbf{K}_n + \sigma^2 \mathbf{I})^{-1}$  and  $\mathbf{f}_n := (y_1, y_2, y_3)^\top$ . (These modifications are theoretically justified; see e.g. Kanagawa et al. (2018) and references therein for details.) The green curves are 5 sample paths from the posterior Gaussian process (3.4)

Matérn-5/2 kernel of the form

$$k(x, x') = \left( 1 + \frac{\sqrt{5}\|x - x'\|}{h} + \frac{5\|x - x'\|^2}{3h^2} \right) \exp \left( -\frac{\sqrt{5}\|x - x'\|}{h} \right) \quad (3.3)$$

where  $h > 0$  is a scale parameter.<sup>6</sup> Roughly, this kernel leads to  $f \sim \mathcal{GP}(0, k)$  that is almost surely twice differentiable (e.g., Kanagawa et al., 2018, Section 4.4). Thus, with this kernel we essentially assume this degree of smoothness for the objective function, and this is our prior assumption.

**Posterior Gaussian process.** The use of a Gaussian process as a prior leads to an *analytic* expression of the resulting posterior distribution. Given data  $D_n = \{(x_i, f(x_i))\}_{i=1}^n$ , the posterior distribution of  $f$  is also given as a Gaussian process

$$f|D_n \sim \mathcal{GP}(m_n, k_n), \quad (3.4)$$

<sup>6</sup>In our simulation study, we use the default value for  $h$  of the mlrMBO package.

where  $\mu_n : \Omega \rightarrow \mathbb{R}$  is the *posterior mean function* and  $k_n : \Omega \times \Omega \rightarrow \mathbb{R}$  is the *posterior covariance function*, given by

$$m_n(x) = \mathbb{E}[f(x)|D_n] = \mathbf{f}_n^\top \mathbf{K}_n^{-1} \mathbf{k}_n(x), \quad x \in \Omega, \quad (3.5)$$

$$\begin{aligned} k_n(x, x') &= \mathbb{E}[(f(x) - m_n(x))(f(x') - m_n(x))|D_n] \\ &= k(x, x') - \mathbf{k}_n(x)^\top \mathbf{K}_n^{-1} \mathbf{k}_n(x'), \quad x, x' \in \Omega, \end{aligned} \quad (3.6)$$

where  $\mathbf{f}_n := (f(x_1), \dots, f(x_n))^\top$ ,  $\mathbf{k}_n(x) := (k(x, x_1), \dots, k(x, x_n))^\top \in \mathbb{R}^n$  and  $\mathbf{K}_n := (k(x_i, x_j))_{i,j=1}^n \in \mathbb{R}^{n \times n}$ . For the detail of the above derivation, see Rasmussen and Williams (2006).

The posterior mean function  $m_n$  in (3.5) is an approximation of the objective function  $f$  based on the data  $D_n$ . It works as a computationally cheaper surrogate model of  $f$ . On the other hand, the *posterior standard deviation*

$$\sigma_n(x) := \sqrt{k_n(x, x)} = \sqrt{\mathbb{E}[(f(x) - \mu_n(x))^2|D_n]} \quad (3.7)$$

quantifies the uncertainty about the unknown function value  $f(x)$ . These  $\mu_n$  and  $\sigma_n$  are the building blocks of the acquisition function, as we will see next.

### 3.3 Acquisition function

We now introduce the concrete form acquisition function  $\alpha(x; D_n)$ . There are many acquisition functions proposed in the literature; see Shahriari et al. (2016, Section IV). Most popular ones include the *EI* (Expected Improvement), *GP-UCB* (Gaussian Process Upper Confidence Bound), and *ES* (Entropy Search). In this paper, we use the EI acquisition function, which is standard and theoretically well studied (Bull, 2011). Let

$$f_n^* := \max_{i=1, \dots, n} f(x_i), \quad x_n^* \in \arg \max\{f(x) \mid x \in \{x_1, \dots, x_n\}\}.$$

be the maximum and the maximizer of the objective function  $f(x)$  over the currently evaluated inputs  $x_1, \dots, x_n$ . The EI acquisition function  $\alpha(x; D_n)$  at  $x$  is defined as the expected improvement of the function value  $f(x)$  over the current maximum  $f_n^*$ , where the expectation is with respect to the posterior Gaussian process (3.4):

$$\begin{aligned} a(x; D_n) &:= \mathbb{E}_{f \sim \mathcal{GP}(\mu_n, k_n)}[\max(f(x) - f_n^*, 0)] \\ &= \underbrace{\sigma_n(x) \phi\left(\frac{\mu_n(x) - f_n^*}{\sigma_n(x)}\right)}_{\text{Exploration}} + \underbrace{(\mu_n(x) - f_n^*) \Phi\left(\frac{\mu_n(x) - f_n^*}{\sigma_n(x)}\right)}_{\text{Exploitation}}, \end{aligned} \quad (3.8)$$

where  $\phi : \mathbb{R} \rightarrow [0, \infty)$  is the probability density function of a standard Gaussian random variable, and  $\Phi : \mathbb{R} \rightarrow [0, 1]$  is its cumulative distribution function:  $\Phi(y) := \int_{-\infty}^y \phi(s) ds, y \in \mathbb{R}$ .

The first term in (3.8) represents the *exploration*, as it becomes large when  $\sigma_n(x)$ , which represents the uncertainty about the function value  $f(x)$ , is large. This is typically the case when  $x$  is far from already evaluated locations  $x_1, \dots, x_n$ . The second in (3.8) represents the *exploitation*, as it becomes large when  $\mu_n(x) - f_n^*$  is large and  $\sigma_n(x)$  is small. This is typically the case when  $x$  is near the current maximizer  $x_n^*$ . Thus, the EI acquisition function naturally balances the exploration-exploitation trade-off, and the next point  $x_{n+1} \in \arg \max_{x \in \Omega} \alpha(x; D_n)$  achieves such a balance.

**Soft constraint for non-bankruptcy.** For the maximization of the expected utility (2.11), we have a constraint on the parameters  $x = (\pi, \theta)$  so that the bankruptcy, defined as  $A(t) \leq 0$ , does not occur for any time point  $t > 0$  and for any realization of the financial market. This hard constraint is difficult to achieve in practice, because of the unboundedness of the Brownian motion defining the financial market. Therefore, in the simulation study we use the following soft constraint: If  $A(t) \leq 0$  happens at any  $t > 0$  for any of 10,000 simulations of the financial market, we set the objective function value to its minimum: i.e.,  $f(x) = 0$ . This encourages BO to avoid selecting parameters close to such  $x = (\pi, \theta)$ .

### 3.4 Demonstration

Figure 3 shows an example of points  $x = (\pi, \theta)$  evaluated by BO for  $\gamma = 10$ . The green points are the  $n_{\text{init}} = 10$  initial design points  $x_1, \dots, x_{n_{\text{init}}}$  generated by Latin hypercube sampling. The total number of evaluated points is  $N = 100$ . The red point is the maximizer  $x_N^*$ , and the blue points are the 10 other second-best parameters (largely overlapping with the red point). For a comparison, we show  $10 \times 10$  grid points. Figure 2 also shows a heat map describing the landscape of the objective function  $f(x) = f(\pi, \theta)$  (red: higher; blue: lower).

Figure 3 shows that the parameters evaluated by BO concentrate in the region around  $\pi = 0.25$ , where the function values are high (as shown in the heat map). In comparison to the  $10 \times 10$  grids, BO uses the same computational budget of 100 evaluations more efficiently by focusing on the region where the function values are high. This example describes the usefulness of BO in simulation studies of a pension system in general, as BO can reduce computational burdens substantially.

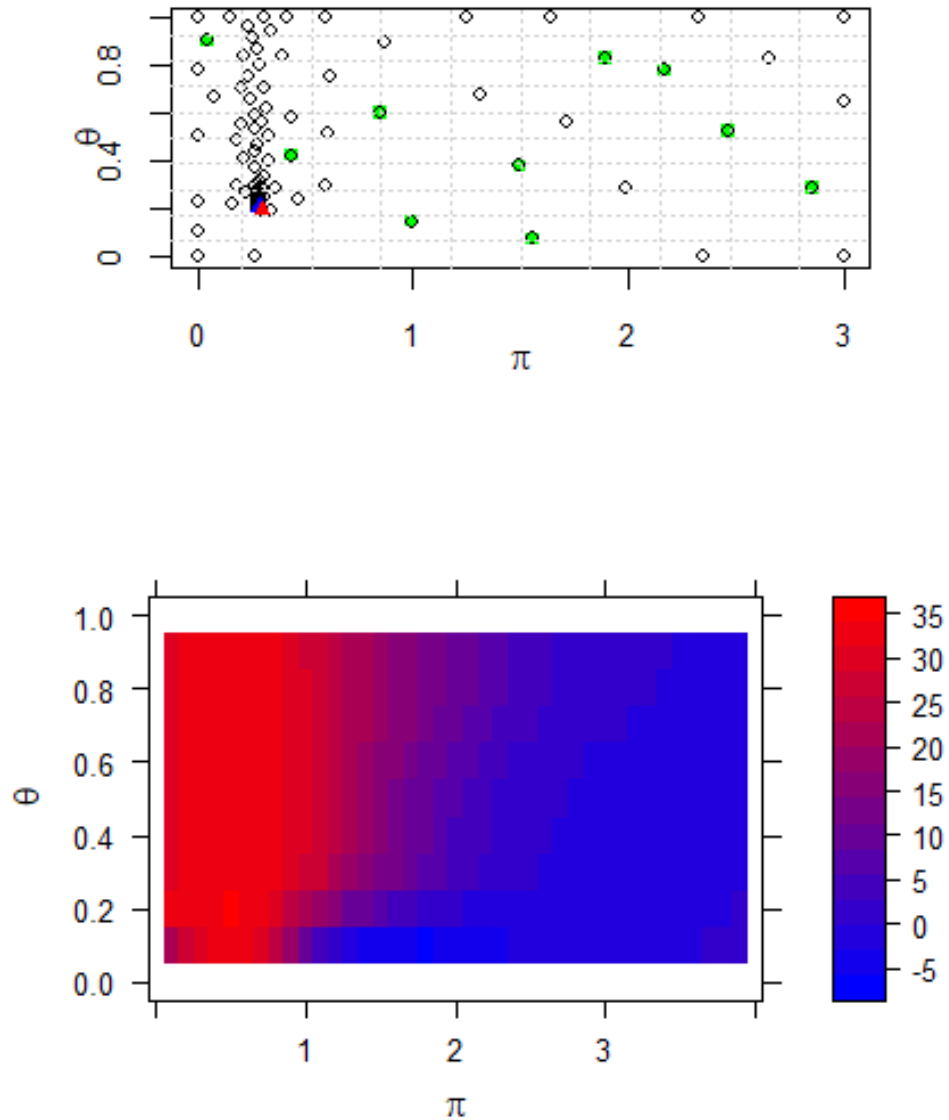


Figure 3: Demonstration of Bayesian optimization with  $\gamma = 10$  (see Section 3.4). **Top**: The points represent the values of  $(\pi, \theta)$  evaluated by Bayesian optimization. The green points are the initial 10 points given by Latin hypercube sampling. The red point is the maximizer found by Bayesian optimization after 100 evaluations, and the blue points (largely overlapping the red point) are the 10 second-best points. **Bottom**: A heatmap representing the response landscape of the objective function (red: higher, blue: lower). Best seen in color.

## 4 Optimal parameters of the pension model

We study here the optimal values for the two parameters of the pension fund (i.e., the investment strategy  $\pi$  and the adjustment parameter  $\theta$  of the declaration rate) nu-

merically obtained with Bayesian optimization, and how these values depend on the relative risk aversion  $\gamma$  of the social planner (or the fund manager) and the market price of risk of the financial market. In Section 4.1, we first describe the setup for our simulation study also for the later sections on welfare analysis. In Section 4.2, we report the optimal values for the two parameters of the pension model in different settings, and the resulting trajectories of the funding-ratio process.

## 4.1 Simulation setup

We explain here a common setup for the following simulation studies.

**Pension setting.** We set the annual contribution of a working generation to be the unit,  $y = 1$ . Each generation starts working at age  $\tau_0 = 25$  and retires at age  $\tau_R = 65$ . Thus, one generation contributes to the pension fund for  $N = \tau_R - \tau_0 = 40$  years.

**Settings of the financial market.** We first define the *market price of risk*. As defined in Section 2.1, we consider a Black-Scholes market, and recall that  $r > 0$  is the rate of the risk-free asset, and  $\mu > r$  and  $\sigma > 0$  are the constant drift and volatility of the risky asset, respectively. Then the the market price of risk can be defined as

$$\rho := (\mu - r) / \sigma$$

i.e., the excess return  $\mu - r$  divided by the volatility  $\sigma$  of the risky asset. Intuitively, the market is tough if  $\rho$  is small, and vice versa.

We consider three settings of  $\mu$ ,  $r$  and  $\sigma$  and write the resulting market as  $M1$ ,  $M2$  and  $M3$ , corresponding to different levels of the market price of risk  $\rho$ .

$$\begin{aligned} M1 : (\mu, r, \sigma) &= (0.065, 0.02, 0.15), & \rho &= 0.3, \\ M2 : (\mu, r, \sigma) &= (0.065, 0.01, 0.25), & \rho &= 0.22, \\ M3 : (\mu, r, \sigma) &= (0.065, 0.01, 0.5), & \rho &= 0.11. \end{aligned}$$

Thus,  $M1$  is the setting with the highest market price of risk among the three settings, and  $M3$  the lowest.

**Expected utility.** We consider different values for the relative risk aversion  $\gamma$  of the CRRA utility function in the expected utility (2.11), and perform simulations for each

value. In this way, we can study the effects of  $\gamma$ , which represents the risk attitude of the social planner, on the optimal investment strategy  $\pi$  and the adjustment parameter  $\theta$  as well as on the resulting operational characteristics of the pension fund. Specifically we consider the set of values  $\{0.5, 1, 2, 3, 5, 10\}$  for  $\gamma$ , motivated by existing studies; see e.g. Mehra and Prescott (1985); Chiappori and Paiella (2011). We set the subjective discount factor in the expected utility (2.11) as  $\beta = 0.98$ .

**Range of the parameters.** As mentioned in Section 3.1, we specify the search space of the two parameters (the investment strategy  $\pi$  and the declaration rate adjustment parameter  $\theta$ ) as  $(\pi, \theta) \in [0, 3] \times [0, 1]$ . Note that  $\pi > 1$  can be interpreted as the pension fund performing borrowing; we allow for such a situation for our simulation experiments for completeness.

**Simulation method and expected utility.** For the simulation of the asset process (2.1), we use a step size  $\Delta = 1/12$  for a time-horizon of  $T = 100$  years (i.e., the simulation is run from  $t = 0$  to  $t = T = 100$ ). This step size  $\Delta = 1/12$  implies that the asset process and the declaration rate are updated on a monthly basis. The initial values for the asset and liability are specified as  $A(0) = L(0) = a_0$ , so that the initial funding-ratio becomes the unity:  $A(0)/L(0) = 1$ . Note that  $a_0$  is the sum of the assets of the entry cohorts at time  $t = 0$ ; see Section 2.4. For a given pair of investment strategy  $\pi$  and adjustment parameter  $\theta$ , the expected utility in (2.11) is approximated as the empirical average of the utilities over 10,000 simulation paths.

**Bayesian optimization.** As described in Section 3, we use Bayesian optimization to numerically search for the optimal values of the two parameters. We set the number of initial points as  $n_{\text{init}} = 10$ , and the total number of evaluations as  $N = 100$ . See Section 3 for details.

## 4.2 Optimal parameters and the funding-ratio process

Table 1 shows the optimal values for the investment strategy  $\pi$  and the adjustment parameter  $\theta$  of the declaration rate, obtained with Bayesian optimization for various settings of relative risk aversion  $\gamma$  and the financial market. We make the following observations.

Table 1: Optimal values for the investment strategy  $\pi$  and the adjustment parameter  $\theta$  of the declaration rate obtained with Bayesian optimization, for different settings of the financial market ( $M1, M2, M3$ ) and the relative risk aversion  $\gamma$  of the social planner.

	$\gamma = 0.5$	$\gamma = 1$	$\gamma = 2$	$\gamma = 3$	$\gamma = 5$	$\gamma = 10$
M1:	$\pi^* = 2.822$ $\theta^* = 0.882$	$\pi^* = 2.310$ $\theta^* = 0.865$	$\pi^* = 1.244$ $\theta^* = 0.598$	$\pi^* = 0.865$ $\theta^* = 0.345$	$\pi^* = 0.560$ $\theta^* = 0.235$	$\pi^* = 0.300$ $\theta^* = 0.197$
M2:	$\pi^* = 1.895$ $\theta^* = 0.830$	$\pi^* = 1.088$ $\theta^* = 0.533$	$\pi^* = 0.643$ $\theta^* = 0.197$	$\pi^* = 0.442$ $\theta^* = 0.125$	$\pi^* = 0.393$ $\theta^* = 0.072$	$\pi^* = 0.158$ $\theta^* = 0.146$
M3:	$\pi^* = 0.544$ $\theta^* = 0.470$	$\pi^* = 0.286$ $\theta^* = 0.344$	$\pi^* = 0.179$ $\theta^* = 0.135$	$\pi^* = 0.119$ $\theta^* = 0.160$	$\pi^* = 0.069$ $\theta^* = 0.209$	$\pi^* = 0.021$ $\theta^* = 1.080 \times 10^{-5}$

**Investment strategy.** Let us first study how the optimal investment strategy  $\pi^*$ , which is the fraction of the pension asset invested in the risky asset, depends on the relative risk aversion  $\gamma$  and the setting of the financial market. For a fixed financial market, the optimal investment strategy  $\pi^*$  becomes smaller as  $\gamma$  increases (i.e., as the social planner becomes more risk-averse), and vice versa. For instance, for the market  $M2$ , we have  $\pi^* = 1.895$  for  $\gamma = 0.5$  and  $\pi^* = 0.158$  for  $\gamma = 10$ .<sup>7</sup> On the other hand, for a fixed relative risk aversion  $\gamma$ , the optimal investment strategy  $\pi^*$  becomes smaller as the market price of risk decreases; recall that  $M3$  is the market with the lowest market price of risk  $\rho = 0.11$  and  $M1$  the highest  $\rho = 0.3$ . These observations regarding  $\pi^*$  align with the meanings of the relative risk aversion and the market price of risk.

**Declaration rate adjustment parameter.** Let us now look at the optimal adjustment parameter  $\theta^*$  of the declaration rate. It tends to co-vary with  $\pi^*$ : for a large  $\pi^*$ , the associated  $\theta^*$  tends to be large (except the setting  $M3$  with  $\gamma = 2, 3, 5$ , in which  $\pi^*$  is not very large). This tendency may be interpreted as: if  $\pi^*$  is large,  $\theta^*$  needs to be also large to stabilize the funding-ratio process.

**Funding-ratio process.** Figure 4 shows the funding-ratio process averaged over 10,000 simulations using the optimal parameters  $(\pi^*, \theta^*)$  from Table 1 for  $\gamma = 3$  and each of the three settings of the financial market. We can observe that the (averaged) funding-ratio process converges to 1 or remains around a value slightly above 1. A similar pattern can be also observed with the optimal parameters in other settings. However, this is not the case if  $\theta$  is too small; in our preliminary simulation experiments, we observe that the pension fund can go easily bankrupt (i.e.,  $A(t) < 0$  occurs at some  $t > 0$ )

<sup>7</sup>Note that  $\pi^* = 1.895$  can be interpreted as: the fund invests the full amount of its asset in the risky asset, and also performs borrowing of the amount of 89.5% of its asset to invest in the risky asset.

if the adjustment parameter  $\theta$  is too small for a given investment strategy  $\pi$ . Hence, we may understand the optimal adjustment parameter  $\theta^*$  as the one that enables the funding-ratio-linked declaration rate to protect the fund from bankruptcy.

Note that the the funding-ratio increases sharply during the first 10 to 20 years of the pension fund. This phenomenon can be attributed to the rapid increase of the benefit accounts of the entry cohorts during the early period of the pension fund, because their assets before joining the pension fund ( $t < 0$ ) develop according to the risk-free rate (See Section 2.4).

Goecke (2013) proves that, for a *self-financing* pension fund using the same funding-ratio-linked declaration rate and a constant mix strategy, the logarithm of the funding ratio follows an Ornstein-Uhlenbeck process whose expectation converges to 0 (i.e., the funding ratio converges to 1) as the operation time tends to infinity. Since our pension design is an OLG model involving discrete jumps of cash flows (i.e., annual contributions and retirement payments), this result of Goecke (2013) is not directly applicable. However, the funding-ratio process shows a similar pattern in our simulations. This suggests the wider applicability of the funding-ratio-linked declaration rate than the self-financing fund considered in Goecke (2013).

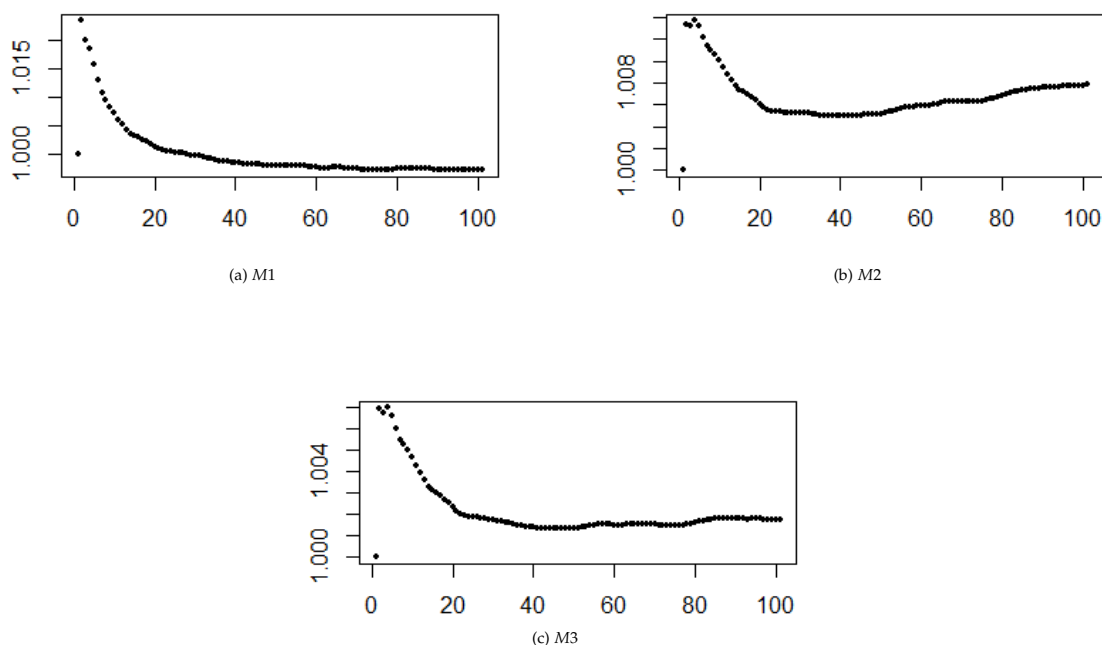


Figure 4: The funding-ratio process averaged over 10,000 simulations using the optimal parameters in Table 1 for  $\gamma = 3$  and for each of the financial market settings,  $M1$ ,  $M2$  and  $M3$ .

This section has studied the optimal parameters under various settings and the result-

ing trajectories of the funding-ratio process. Note that these parameters are optimal from the viewpoint of the social planner running the fund, since they are the (numerical) maximizer of the expected utility of this social planner. While this expected utility takes into account the benefits of all the generations including those from the future, it does not directly provide us with insights into the welfare of individual participants. In the next section, we turn our attention to the resulting retirement benefits of individual participants, and how intergenerational risk sharing works for protecting the participants' assets.

## 5 Welfare analysis and intergenerational risk sharing

This section analyses the welfare of each generation in the pension fund, with a focus on how intergenerational risk sharing (IRS) works. We do this by running simulations using the optimal parameters in Table 1 obtained for various settings in the previous section. To understand the functionality of IRS in our CDC pension model, we also consider the corresponding model for an individual defined-contribution (IDC) plan in which IRS is not implemented. We compare the benefit account of an individual participant in the CDC model and that of the corresponding participant in the IDC model. By studying how they differ, we can elucidate the mechanism of IRS.

Our focus is to understand the functionality of IRS implemented through the funding-ratio-linked declaration rate in our CDC pension model. For this purpose, we assume that an IDC participant under comparison uses the same investment strategy  $\pi$  as the CDC pension fund, so that the only difference between the CDC and IDC benefit accounts is the existence of IRS. As for the CDC participants, we use the number  $i \in \mathbb{N}$  as an indicator of the participant (or generation) in the IDC plan who starts working at time  $i - (\tau_R - \tau_0) = i - 40$  and retires at time  $t = i$ . Let  $A_i(t)$  denote the benefit account of the IDC participant  $i$  at time  $t \in [i - (\tau_R - \tau_0), i]$ , where  $\tau_R = 65$ . Then its dynamics is given by

$$\begin{aligned} A_i(i + \tau_R - \tau_0) &= 0, \\ dA_i(t) &= A_i(t) [(\pi(\mu - r) + r)dt + \pi\sigma dW(t)], \quad t \in [i - (\tau_R - \tau_0), i], \\ A_i(t)_+ &= A_i(t) + y, \quad t \in [i - (\tau_R - \tau_0), i - 1] \cap \mathbb{N}. \end{aligned}$$

That is, the IDC participant  $i$  accumulates the contribution  $y$  annually in her account for  $N = 40$  years (the third line), and the account evolves according to the continuous dynamics determined by her constant mix investment strategy  $\pi \geq 0$  in the financial

market (the second line). Her lump-sum retirement benefit is given by her account value at the time of retirement  $t = i$ , i.e.,  $A_i(i)$ .

We make comparisons between the individual benefit accounts  $B_i(t)$  in the CDC pension model and the corresponding accounts  $A_i(t)$  in the IDC model. In Section 5.1, we first study the stability of the development of each benefit account. In Section 5.2, we make comparisons regarding the retirement benefits.

In the following, we may refer to our pension model as “CDC” (collective defined-contribution) in contrast to the IDC model.

## 5.1 Stability of individual benefit accounts

We first study how each individual benefit account evolves over time by simulating its path. As mentioned, the CDC uses the optimal parameters  $\pi^*$  and  $\theta^*$  in Table 1, and the corresponding IDC plan uses the same investment strategy  $\pi^*$ . In Figure 5, We show some examples of simulated paths of the CDC account  $B_i(t)$  and the corresponding IDC  $A_i(t)$  of generation  $i = 41$  (i.e., the generation who starts working at time  $t = 1$  and retires at time  $t = 41$ ) for  $\gamma = 3$  and for the three financial market settings. Note that each account lasts for 40 years = 480 months. More examples are given in Appendix A.

We can observe that, for each case, the CDC account evolves more smoothly than the corresponding IDC account. This smoothness of the CDC account comes from inter-generational risk sharing, since the only difference between the CDC and IDC accounts is the declaration rate process in the CDC pension model. These results show that the funding-ratio-linked declaration adds more stability to the individual benefit accounts in the CDC pension system.

To quantitatively assess the smoothness of each path, we calculate the *increment-ratio-based roughness (IR-roughness)*, a measure of smoothness for a stochastic process (Bardet et al., 2011).<sup>8</sup> To describe the IR-roughness measure, we suppose that the path of each benefit account is represented by a function  $g : [0, T] \rightarrow \mathbb{R}$ , where  $T > 0$  is its terminal time. Discretizing the domain to  $n - 1 \in \mathbb{N}$  intervals, the first-order IR-roughness is

---

<sup>8</sup>One may consider calculating the variance of each simulation path  $g : [0, T] \rightarrow \mathbb{R}$  defined by  $\frac{1}{T} \int_0^T (g(t) - m_g)^2 dt$  with the mean  $m_g = \frac{1}{T} \int_0^T g(t) dt$  (or its discrete approximation), but this variance does not provide an informative measure of smoothness. This is because the value of the variance is mostly determined by the upward trend of each path. For example, the mean  $m_g$  of either CDC or IDC paths in Figure 5 (a) is around 100, and the path increases from 0 to around 200. Compared to this upward trend, the fluctuations of either path is relative smaller and thus the resulting variance does not capture these fluctuations. Therefore we use the IR-roughness as a measure of smoothness.

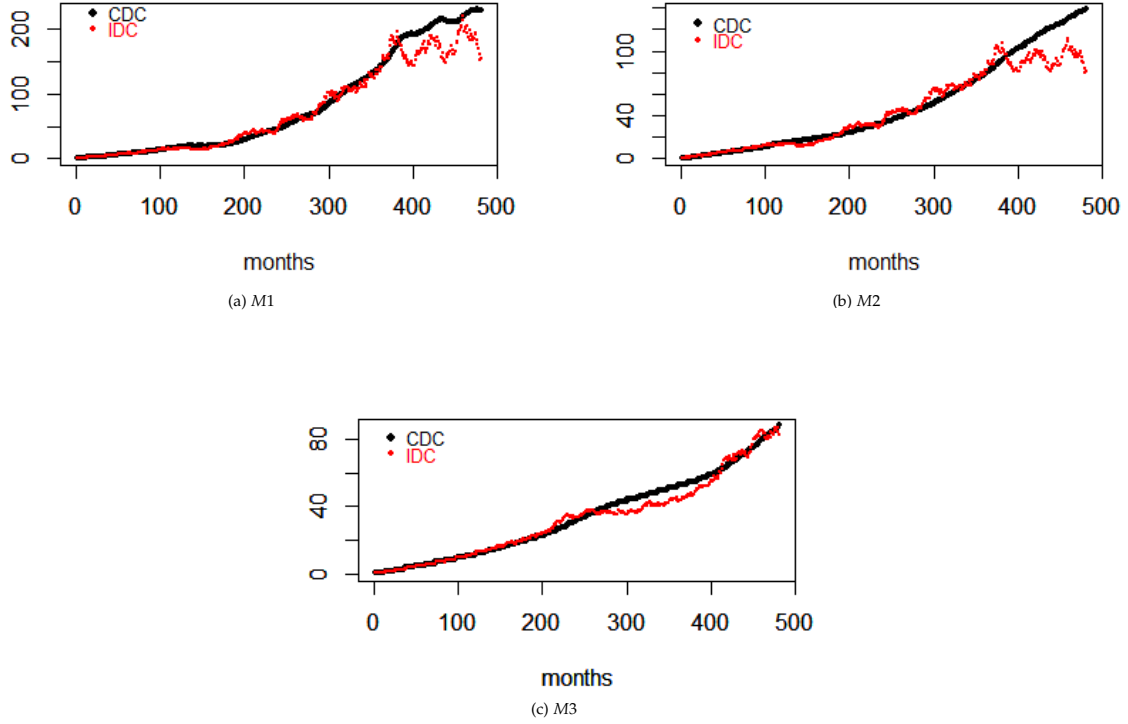


Figure 5: Examples of simulated trajectories of the CDC (black) and IDC (red) accounts of generation  $i = 41$  for  $\gamma = 3$  and for the three settings of the financial market ( $M_1$ ,  $M_2$  and  $M_3$ ).

defined as

$$R^{1,n}(g) := \frac{1}{n-1} \sum_{j=0}^{n-2} \frac{\left| g(T^{j+1}/n) - g(T^j/n) + g(T^{j+2}/n) - g(T^{j+1}/n) \right|}{\left| g(T^{j+1}/n) - g(T^j/n) \right| + \left| g(T^{j+2}/n) - g(T^{j+1}/n) \right|}. \quad (5.1)$$

By the triangle inequality, the numerator in the sum is less than or equal to the denominator, and thus  $R^{1,n}(g)$  takes values between 0 and 1. When the signs of the two increments  $g(T(j+1)/n) - g(Tj/n)$  and  $g(T(j+2)/n) - g(T(j+1)/n)$  are the same, the numerator equals the denominator, while when those signs are different, the numerator is smaller than the denominator. As such,  $R^{1,n}(g)$  reflects the sign changes of the function  $g$  and thus quantifies its roughness. Intuitively,  $R^{1,n}(g)$  is close to 0 when  $g$  is rough, and is close to 1 when  $g$  is smooth. In fact, Bardet et al. (2011) show that, for a sufficiently smooth  $g$ ,  $R^{1,n}(g)$  converges to 1 as  $n \rightarrow \infty$ .

Tables 2 reports the IR-roughness of the CDC and IDC accounts of generation  $i = 41$ , averaged over 10,000 simulation paths, for different settings of the financial market and relative risk aversion  $\gamma$ . For each setting, the IR-roughness of the CDC is larger than the IDC, and this implies that the CDC account evolves more smoothly than the

corresponding IDC account on average.

Table 2: IR roughness measure for the CDC and IDC accounts of generation  $i = 41$ , averaged over 10,000 paths.

		$\gamma = 0.5$	$\gamma = 1$	$\gamma = 2$	$\gamma = 3$	$\gamma = 5$	$\gamma = 10$
M1	CDC	0.933	0.934	0.950	0.972	0.988	1.000
	IDC	0.723	0.724	0.728	0.731	0.737	0.750
M2	CDC	0.927	0.942	0.974	0.987	0.994	0.994
	IDC	0.722	0.724	0.727	0.731	0.732	0.747
M3	CDC	0.941	0.957	0.982	0.984	0.987	1.000
	IDC	0.723	0.727	0.732	0.738	0.748	0.777

## 5.2 Comparison of retirement benefits

We now compare the retirement benefits of the CDC participants and those of the corresponding IDC participants, to investigate how IRS affects the retirement benefits. As we simulate our CDC pension model for 100 years, there are 61 generations whose working periods are contained in the 100 operating years of the pension fund (i.e., generations  $i = 40, \dots, 100$ ; recall that generation  $i$  is those who retire at time  $t = i$ ). We study the retirement benefits of these generations.

### 5.2.1 Quantile values of retirement benefits

Figure 6 shows the median values of the retirement benefits over 10,000 simulations for generation  $i = 40, 41, \dots, 100$ , for each of the CDC and IDC plans, under different settings of the financial market and relative risk aversion  $\gamma$ . (Other settings of  $\gamma$  are shown in Appendix B.) In most cases, the retirement benefits of the IDC are higher than the CDC. The difference between the IDC and CDC is relatively larger for more risky investment strategies ( $\gamma = 0.5$ ), but the difference is smaller for less risky investment strategies  $\gamma = 3, 10$  and in particular for the tough market M3.

Figure 7 describes the corresponding lower 1% quantile values of the retirement benefits over 10,000 simulations (other cases of  $\gamma$  are shown in Appendix C). These are the worst scenarios, and the trend is different from Figure 6: *In many cases, in particular in relatively tough markets (M2 and M3) with low market prices of risk, the CDC retirement benefits are higher than the corresponding IDC retirement benefits.* These results indicate that *intergenerational risk sharing with the funding-ratio-linked declaration rate works well*

for protecting the CDC participants from losing too much, in the worst scenarios of a tough market. (Recall that the only difference between the CDC and IDC models here is the existence of the declaration rate process in the CDC model).

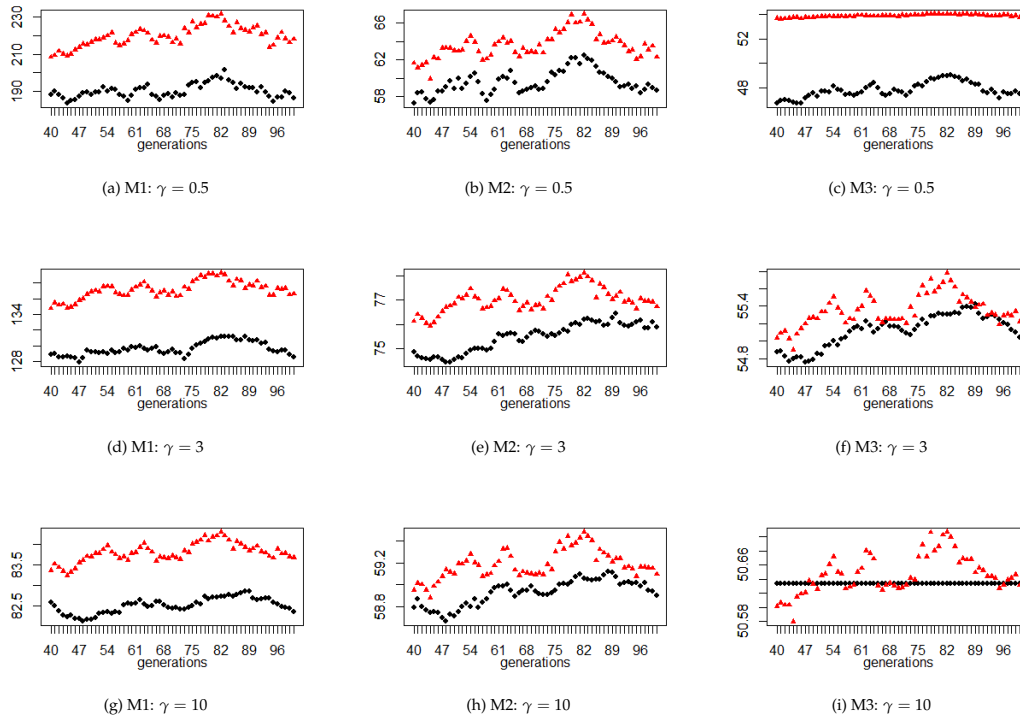


Figure 6: Median values of retirement benefits over 10,000 simulations (Black: CDC; Red: IDC). The subfigures show results for different settings of the financial market ( $M1$ ,  $M2$ ,  $M3$ ) and the relative risk aversion  $\gamma = 0.5, 3, 10$  of the social planner running the pension fund. In each subfigure, the horizontal axis indicates different generations  $i = 40, 41, \dots, 100$ , and the vertical axis shows their retirement benefits.

To support the above findings, we show in Figure 8 the left tail region of the (empirical) cumulative distribution function of the retirement benefits of generation  $i = 41$  over 10,000 simulations, for the three settings of the financial market and relative risk aversion  $\gamma = 3$ . (Results for other settings are given in Appendix D). For the relatively tough financial markets  $M2$  and  $M3$ , the cumulative distribution function for the IDC is higher than the CDC in the left tail region. This implies that there exist many more cases in 10,000 simulations where the IDC retirement benefits are lower than the CDC in the worst scenarios. Hence, the CDC participants are better protected in the worst scenarios of the tough markets with low market prices of risk. The trend is the opposite in the financial market  $M1$ , where the market price of risk is higher.

To summarize, our main finding is: *intergenerational risk sharing via the declaration rate adjustment works for protecting the CDC pension participants from losing too much in the worst scenarios of a tough market.* We argue that this functionality of intergenerational

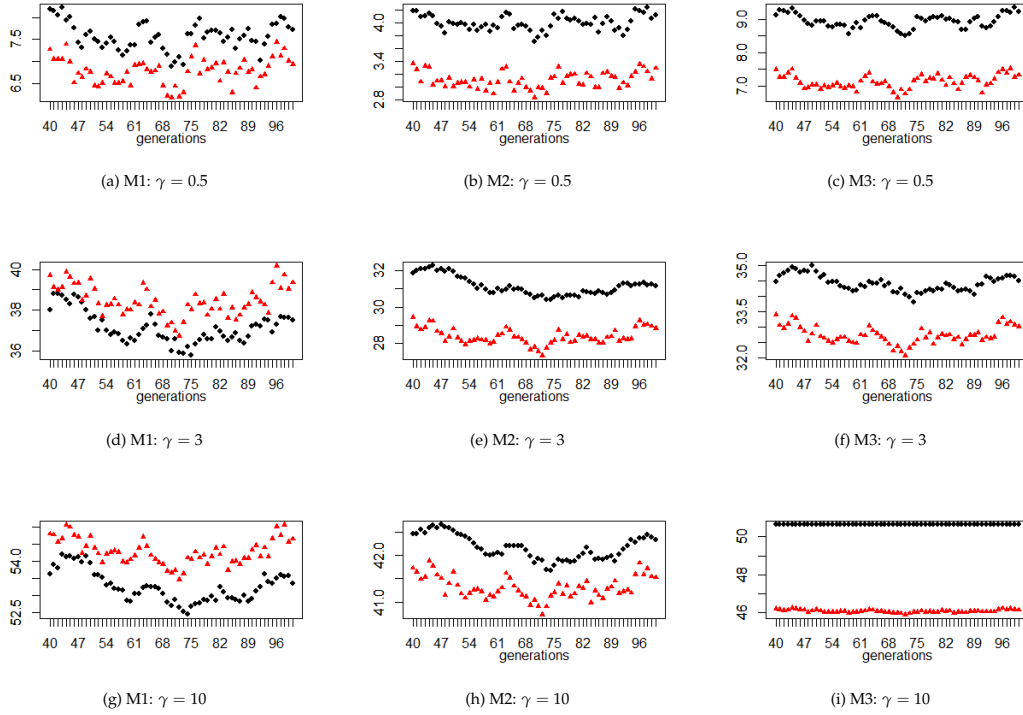


Figure 7: Lower 1% quantile values of retirement benefits over 10,000 simulations (Black: CDC; Red: IDC). The subfigures show results for different settings of the financial market ( $M1$ ,  $M2$ ,  $M3$ ) and the relative risk aversion  $\gamma = 0.5, 3, 10$  of the social planner running the pension fund. In each subfigure, the horizontal axis indicates different generations  $i = 40, 41, \dots, 100$ , and the vertical axis shows their retirement benefits.

risk sharing is important, since it makes the pension system robust against the worst-case scenarios of the financial market. Such robustness is particularly desirable for public pension systems.

### 5.2.2 Certainty equivalents

We study here the welfare of pension participants in terms of the certainty equivalents of their expected utility levels. For simplicity, we assume that each participant has the same CRRA utility function  $U_\gamma$  in (2.10) as that of the social planner managing the pension fund. While this is not necessarily true in reality, we make this assumption to focus on the effects of intergenerational risk sharing.

For each generation  $i = 40, 41, \dots, 100$ , recall that  $B_i(i)$  and  $A_i(i)$  are the retirement benefits when participating the CDC and IDC pension plans, respectively; see Section 2.2 and the begging of Section 5. Then, the corresponding certainty equivalents with the CDC and IDC plans, denoted respectively by  $CE_i^{(CDC)} \geq 0$  and  $CE_i^{(IDC)} \geq 0$ , are

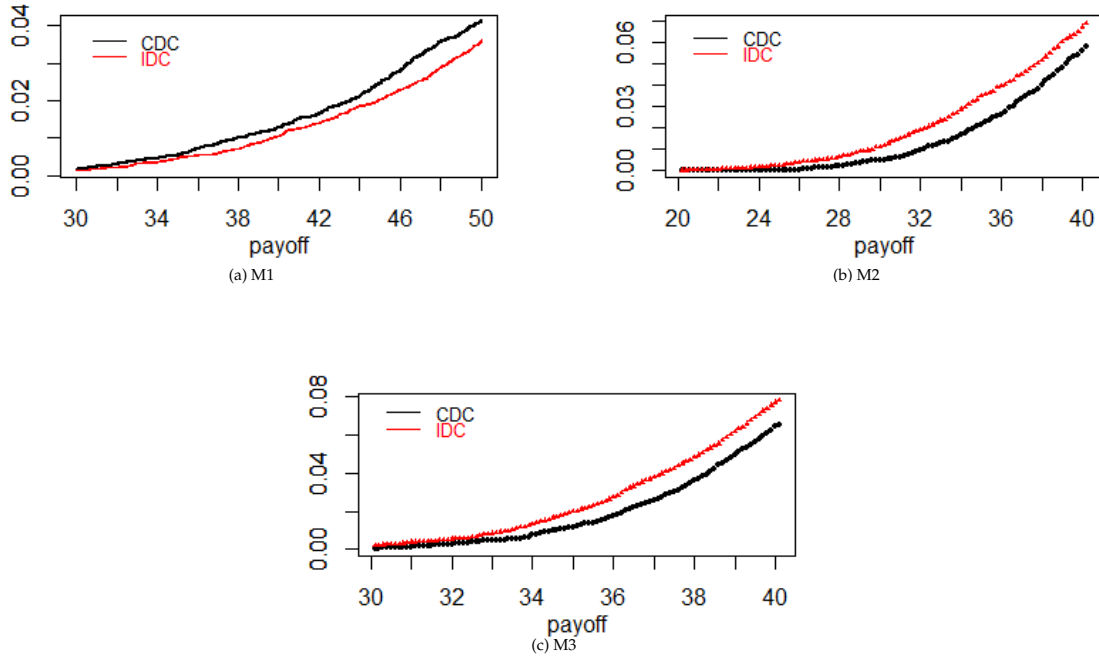


Figure 8: Left tail region of the (empirical) cumulative distribution function of the retirement benefits over 10,000 simulations of generation  $i = 41$ , for the three settings of the financial market ( $M1$ ,  $M2$  and  $M3$ ) and relative risk aversion  $\gamma = 3$  (Black: CDC; Red: IDC). The horizontal axis indicates the amount of retirement benefits (payoffs), and the vertical axis is the value of the cumulative distribution function.

defined by

$$U_\gamma(CE_i^{(CDC)}) = \mathbb{E}[U_\gamma(B_i(i))], \quad U_\gamma(CE_i^{(IDC)}) = \mathbb{E}[U_\gamma(A_i(i))],$$

where, as before, we approximate each expectation by 10,000 simulations.

Figure 9 shows the computed certainty equivalents for different settings of the financial market and relative risk aversion  $\gamma$ . (Results for other settings are given in Appendix E). Consistent with our findings so far, the certainty equivalents of the CDC participants are higher than the corresponding IDC in tough markets ( $M2$  and  $M3$ ) with low market prices of risk, and the opposite trend is observed for the market with a high market price of risk ( $M1$ ). Since the only difference between the CDC and IDC plans is the declaration rate process in the CDC, these results suggest that intergenerational risk sharing of the CDC via the declaration rate adjustment works for improving the participants' welfare in a tough market.

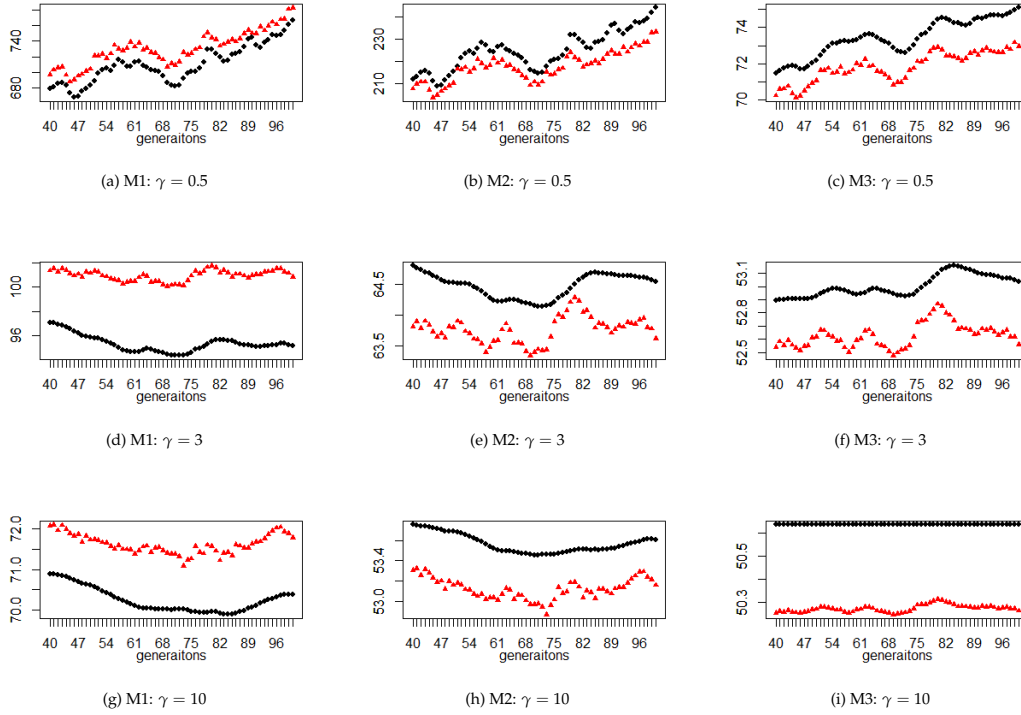


Figure 9: Certainty equivalents of the CDC and IDC participants for generations  $i = 40, 41, \dots, 100$  for different settings of the financial market (M1, M2 and M3) and the relative risk aversion  $\gamma$  (Black: CDC; Red: IDC). The horizontal axis indicates different generations, and the vertical axis shows the values of their certainty equivalents.

## 6 Conclusions

We investigate the functionality of intergenerational risk sharing (IRS) in a CDC pension model, implemented through the funding-ratio-linked declaration rate process. Our main findings, obtained by comparisons to the corresponding IDC pension model, are that 1) IRS makes the development of each individual benefit account more stable, and that 2) IRS protects the participants from losing too much in the worst scenarios of a tough financial market. These characteristics of IRS are promising for public pension systems, since they make the pension fund robust against possible worst-case scenarios.

There are several possible future directions. Since our work is based on simulations, it is straightforward to extend our stylized model to a more realistic one. For instance, one may consider a more detailed realistic model for the entry cohorts, which is important for studying the early phase of the pension fund. Similarly, one can study the pension system in more realistic models for the financial market other than the Black-Scholes model, e.g., those with fat tails.

Our extensive simulation study is enabled by the use of Bayesian optimization for numerically searching for the optimal parameters in the pension model. Bayesian optimization is much more efficient than traditional brute-force approaches such as grid search, and has been widely used in many areas of science and engineering. In this work, we demonstrate the usefulness of Bayesian optimization in simulation studies of a pension system. We believe that our work can encourage the use of Bayesian optimization, or more generally machine learning techniques, in pension research, opening up many possibilities for studying more realistic but computationally intensive pension models.

# A Simulated paths of individual benefit accounts

Figure 10 describes supplementary results for the simulation experiments in Section 5.1 (Figure 5).

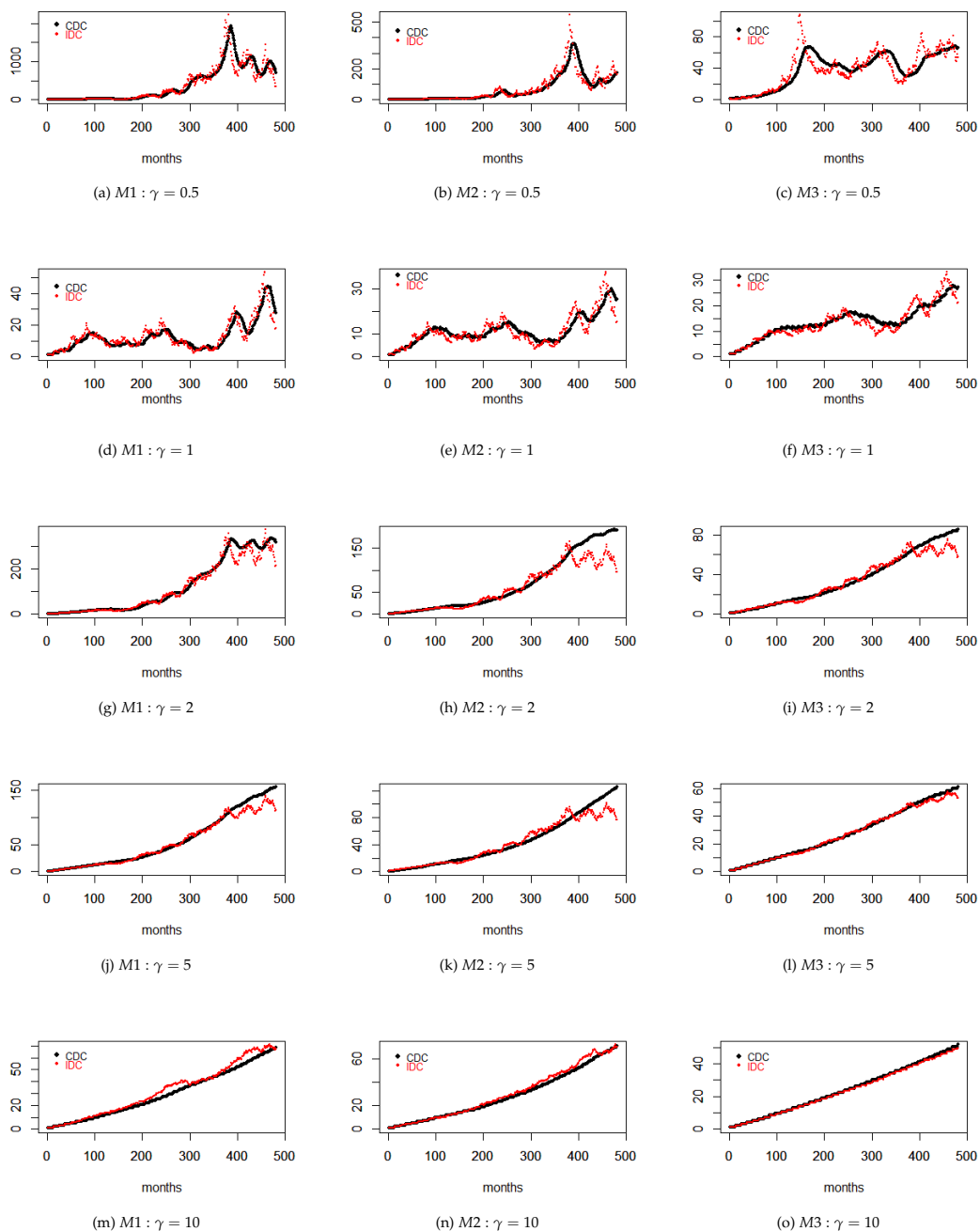


Figure 10: Examples of simulated trajectories of the CDC (black) and IDC (red) accounts of generation  $i = 41$  for relative risk aversion  $\gamma \in \{0.5, 1, 2, 5, 10\}$  and for the three settings of the financial market ( $M_1$ ,  $M_2$  and  $M_3$ ).

## B Median values of retirement benefits

Figure 11 describes supplementary results for the simulation experiments in Section 5.2.1 (Figure 6).

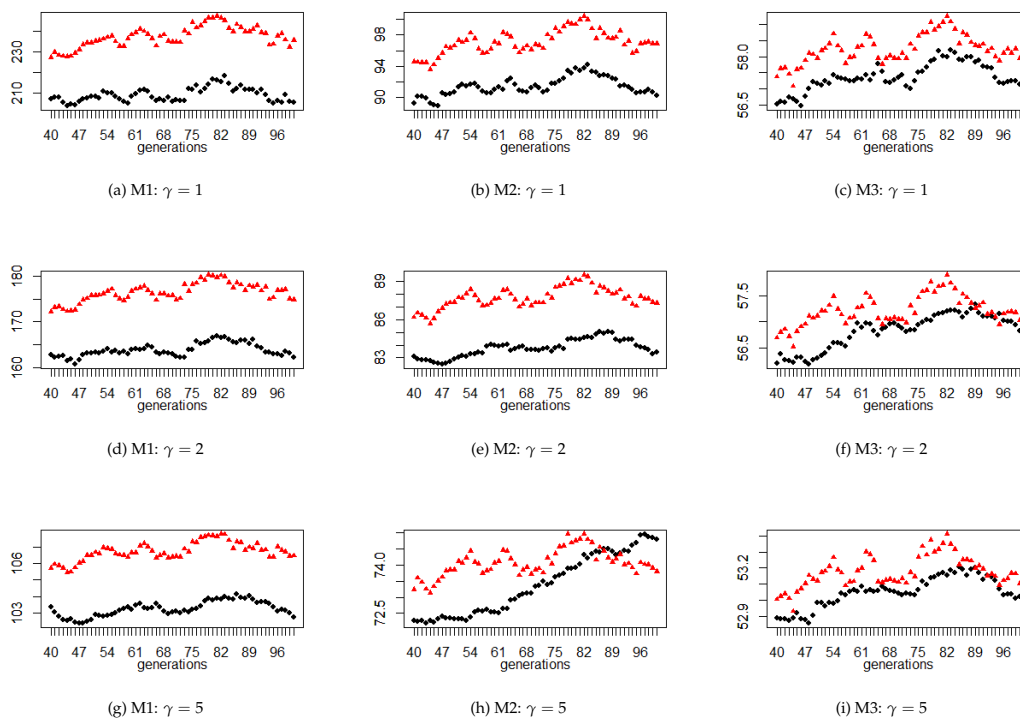


Figure 11: Median values of retirement benefits over 10,000 simulations (Black: CDC; Red: IDC). The subfigures show results for different settings of the financial market ( $M1$ ,  $M2$ ,  $M3$ ) and the relative risk aversion  $\gamma \in \{1, 2, 5\}$  of the social planner running the pension fund. In each subfigure, the horizontal axis indicates different generations  $i = 40, 41, \dots, 100$ , and the vertical axis shows their retirement benefits.

## C Lower 1% quantile values of retirement benefits

Figure 12 describes supplementary results for the simulation experiments in Section 5.2.1 (Figure 7).

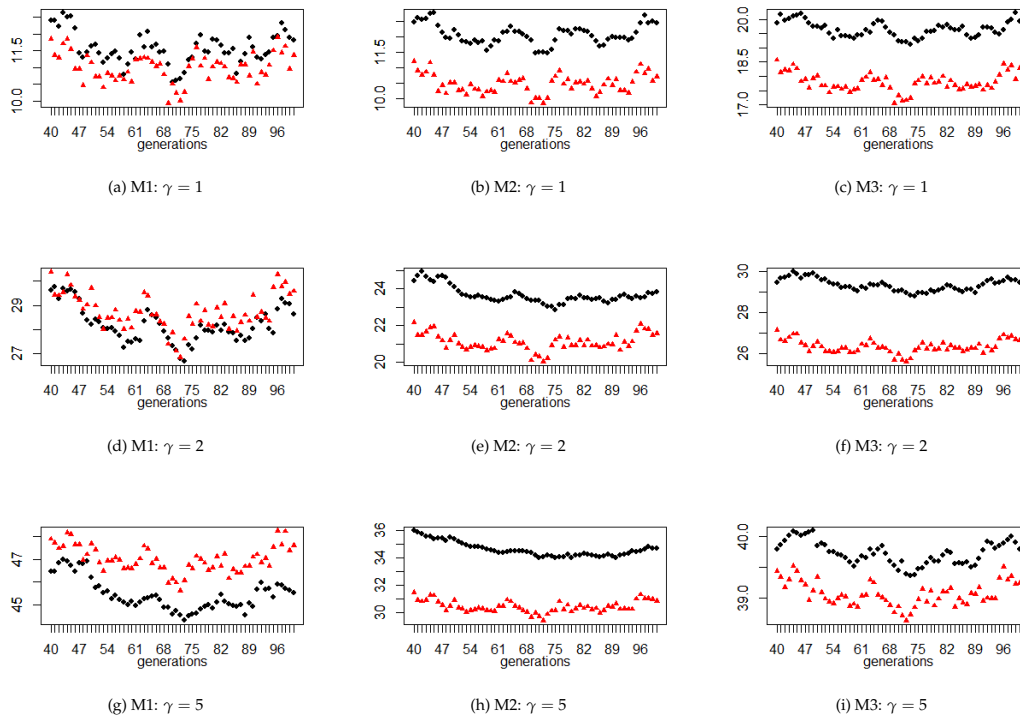


Figure 12: Lower 1% quantile values of retirement benefits over 10,000 simulations (Black: CDC; Red: IDC). The subfigures show results for different settings of the financial market ( $M1$ ,  $M2$ ,  $M3$ ) and the relative risk aversion  $\gamma \in \{1, 2, 5\}$  of the social planner running the pension fund. In each subfigure, the horizontal axis indicates different generations  $i = 40, 41, \dots, 100$ , and the vertical axis shows their retirement benefits.

## D Left tail region of the cumulative distribution of retirement benefits

Figure 13 describes supplementary results for the simulation experiments in Section 5.2.1 (Figure 8).

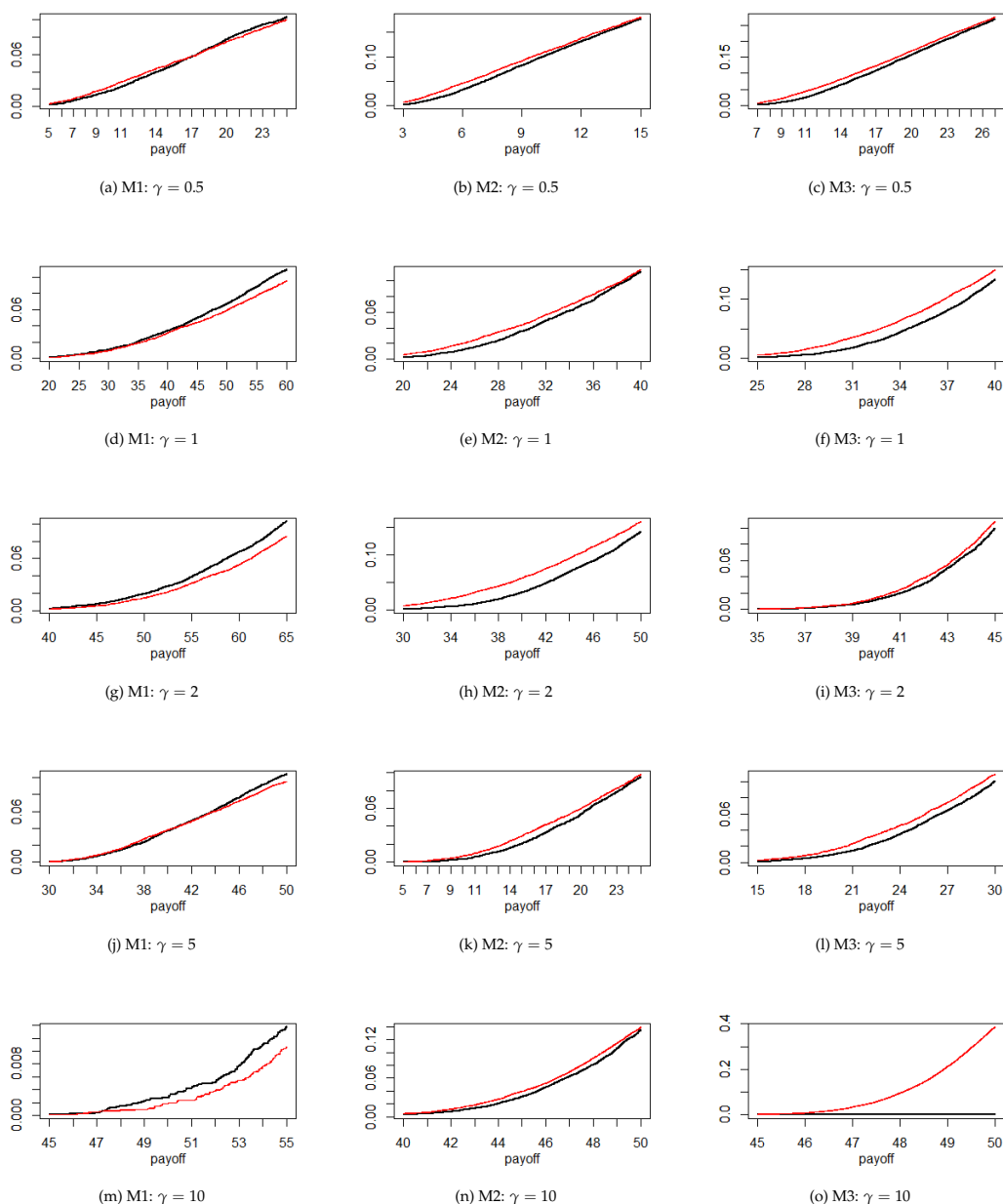


Figure 13: Left tail region of the (empirical) cumulative distribution function of the retirement benefits over 10,000 simulations of generation  $i = 41$ , for the three settings of the financial market (M1, M2 and M3) and relative risk aversion  $\gamma \in \{0.5, 1, 2, 5, 10\}$  (Black: CDC; Red: IDC). The horizontal axis indicates the amount of retirement benefits (payoffs), and the vertical axis is the value of the cumulative distribution function.

## E Certainty equivalents of pension participants

Figure 14 describes supplementary results for the simulation experiments in Section 5.2.2 (Figure 9).

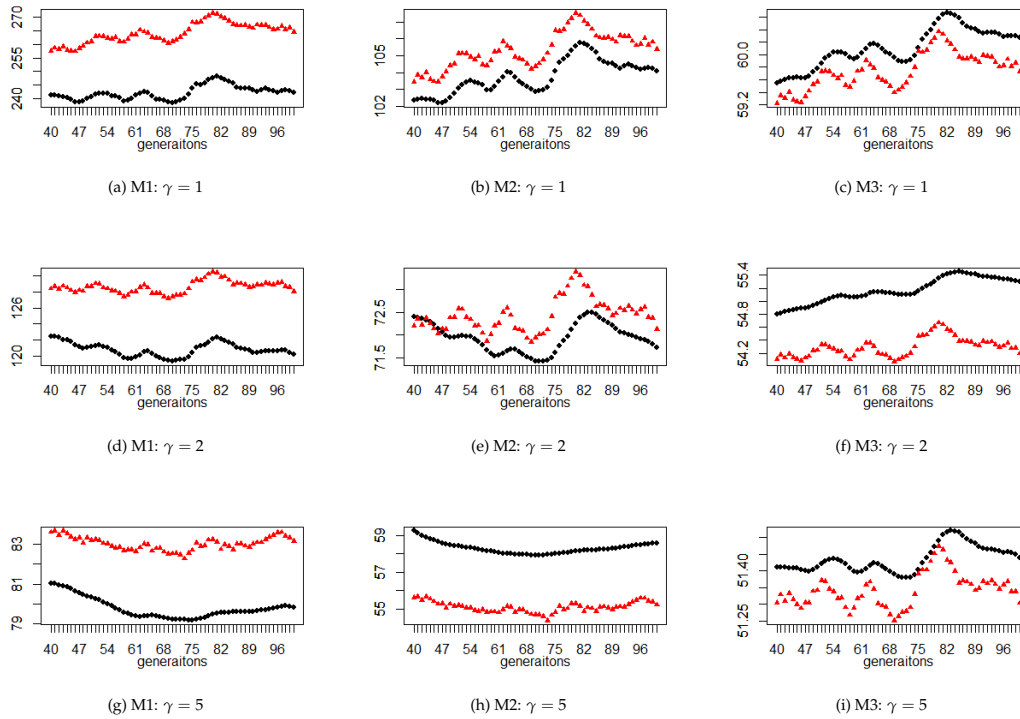


Figure 14: Certainty equivalents of the CDC and IDC participants for generations  $i = 40, 41, \dots, 100$  for different settings of the financial market ( $M1$ ,  $M2$  and  $M3$ ) and the relative risk aversion  $\gamma \in \{1, 2, 5\}$  (Black: CDC; Red: IDC). The horizontal axis indicates different generations, and the vertical axis shows the values of their certainty equivalents.

## References

- Bams, D., Schotman, P. C., and Tyagi, M. (2016). Optimal risk sharing in a collective defined contribution pension system. *Netspar Discussion Paper*.
- Bardet, J.-M., Surgailis, D., et al. (2011). Measuring the roughness of random paths by increment ratios. *Bernoulli*, 17(2):749–780.
- Baumann, R. T. and Müller, H. H. (2008). Pension funds as institutions for intertemporal risk transfer. *Insurance: Mathematics and Economics*, 42(3):1000–1012.
- Beetsma, R. M. and Bovenberg, A. L. (2009). Pensions and intergenerational risk-sharing in general equilibrium. *Economica*, 76(302):364–386.
- Benartzi, S. and Thaler, R. H. (2001). Naive diversification strategies in defined contribution saving plans. *American Economic Review*, 91(1):79–98.
- Bischl, B., Richter, J., Bossek, J., Horn, D., Thomas, J., and Lang, M. (2017). mlrmb: A modular framework for model-based optimization of expensive black-box functions. *arXiv preprint arXiv:1703.03373*.
- Bodie, Z., Marcus, A. J., and Merton, R. C. (1988). Defined benefit versus defined contribution pension plans: What are the real trade-offs? In *Pensions in the US Economy*, pages 139–162. University of Chicago Press.
- Bovenberg, L., Koijen, R., Nijman, T., and Teulings, C. (2007). Saving and investing over the life cycle and the role of collective pension funds. *De Economist*, 155(4):347–415.
- Bovenberg, L. and Nijman, T. (2019). New dutch pension contracts and lessons for other countries. *Journal of Pension Economics and Finance*, 18(3):331–346.
- Broeders, D., Chen, A., and Rijsbergen, D. (2013). Valuation of liabilities in hybrid pension plans. *Applied Financial Economics*, 23(15):1215–1229.
- Bull, A. D. (2011). Convergence rates of efficient global optimization algorithms. *Journal of Machine Learning Research*, 12:2879–2904.
- Chen, A. and Delong, L. (2015). Optimal investment for a defined-contribution pension scheme under a regime switching model. *ASTIN Bulletin: The Journal of the IAA*, 45(2):397–419.

- Chen, A. and Uzelac, F. (2015). Portability, salary and asset price risk: A continuous-time expected utility comparison of db and dc pension plans. *Risks*, 3(1):77–102.
- Chiappori, P.-A. and Paiella, M. (2011). Relative risk aversion is constant: Evidence from panel data. *Journal of the European Economic Association*, 9(6):1021–1052.
- Copeland, C. (2011). Target-date fund use in 401 (k) plans and the persistence of their use, 2007-2009. *EBRI Issue Brief*, (361).
- Cui, J., De Jong, F., and Ponds, E. (2011). Intergenerational risk sharing within funded pension schemes. *Journal of Pension Economics and Finance*, 10(1):1–29.
- Diamond, P. A. (1977). A framework for social security analysis. *Journal of Public Economics*, 8(3):275–298.
- Donnelly, C. (2017). A discussion of a risk-sharing pension plan. *Risks*, 5(1):12.
- Goecke, O. (2013). Pension saving schemes with return smoothing mechanism. *Insurance: Mathematics and Economics*, 53(3):678–689.
- Gollier, C. (2008). Intergenerational risk-sharing and risk-taking of a pension fund. *Journal of Public Economics*, 92(5-6):1463–1485.
- Gordon, R. H. and Varian, H. R. (1988). Intergenerational risk sharing. *Journal of Public Economics*, 37(2):185–202.
- Kanagawa, M., Hennig, P., Sejdinovic, D., and Sriperumbudur, B. K. (2018). Gaussian processes and kernel methods: A review on connections and equivalences. *arXiv preprint arXiv:1807.02582*.
- Kessler, A. (2019). New solutions to an age-old problem: innovative strategies for managing pension and longevity risk. *North American Actuarial Journal*, pages 1–18.
- Kurtbegu, E. (2018). Replicating intergenerational longevity risk sharing in collective defined contribution pension plans using financial markets. *Insurance: Mathematics and Economics*, 78:286–300.
- Lin, Y., MacMinn, R. D., and Tian, R. (2015). De-risking defined benefit plans. *Insurance: Mathematics and Economics*, 63:52–65.
- McKay, M. D., Beckman, R. J., and Conover, W. J. (2000). A comparison of three methods for selecting values of input variables in the analysis of output from a computer code. *Technometrics*, 42(1):55–61.

- Mehra, R. and Prescott, E. C. (1985). The equity premium: A puzzle. *Journal of Monetary Economics*, 15(2):145–161.
- Nijman, T. et al. (2014). Pension reform in the Netherlands: Attractive options for other countries? *Bankers, Markets and Investors*, (128):36–45.
- OECD (2020). Annual survey of investment regulations of pension funds and other pension providers, 2020.
- Poterba, J., Rauh, J., Venti, S., and Wise, D. (2007). Defined contribution plans, defined benefit plans, and the accumulation of retirement wealth. *Journal of Public Economics*, 91(10):2062–2086.
- Rasmussen, C. and Williams, C. (2006). *Gaussian Processes for Machine Learning*. MIT Press.
- Shahriari, B., Swersky, K., Wang, Z., Adams, R. P., and De Freitas, N. (2016). Taking the human out of the loop: A review of Bayesian optimization. *Proceedings of the IEEE*, 104(1):148–175.
- Shiller, R. J. (1999). Social security and institutions for intergenerational, intragenerational, and international risk-sharing. In *Carnegie-Rochester Conference Series on Public Policy*, volume 50, pages 165–204. Elsevier.
- Westerhout, E. (2020). Pension reform in the Netherlands. *CentER Discussion Paper*.